Original Research Article||

Characteristics of Soils Types along the Toposequence in Central Highlands of Ethiopia

Haymanot Awgchew[1*], Sheleme Beyene[1], Alemayehu Kiflu[1]

[1]*School of Plant and Horticultural Science, Hawassa University, Ethiopia*

Abstract

It is imperative to understand and predict the nature and distribution of soils along a given physiographic condition. However, the hitherto practices of collecting basic soil information at a site-specific level seem inadequate to ensure sustainable agricultural production via proper utilization and effective management of soil resources. Therefore, this research was conducted to characterize, classify, and map soils along the toposequence of the Qenberenaweti sub-watershed, Central Highlands of Ethiopia. A total of 91 auger inspections were made up to a 120 cm depth to define soil mapping units with their boundaries. Then, six pedons were opened at typical slope positions along the toposequence. The depth of the pedons varied between 135 and 200+ cm, whereas the thickness of A-horizons showed an increasing trend down the slope by excluding the back-slope position. All the soils at the surface and subsurface horizons had clayey texture with pH ranging from 5.59 to 6.23 and 5.31 to 7.65, respectively. The OC contents throughout the entire horizons varied from 0.22 to 2.03%. The highest CEC values were found at the middle slope position followed by pedons at the upper and bottom parts. The exchangeable cations of most pedons were in declining order of Ca, Mg, K, and Na except for the Mg dominance over Ca at the back slope and bottom depression. Hereby, six soil types were identified; and their distribution was mapped. The results of this research revealed that the extent of variations in key topographic features resulted in the formation, development, and distribution of diversified soils along the toposequence. Consequently, such detailed soil characterization, classification, and mapping work is vital for proper planning, management, and utilization of the soil resources at local topographic conditions. However, further research should be done to ensure sustainable agricultural production in the study area.

Key words: Topography, Soil Mapping Unit, Pedon, Horizon, Soil Properties.

Original submission: August 19, 2024; **Revised submission**: October 28, 2024; **Published online**: November 21, 2024

***Corresponding author's address:** Haymanot Awgchew, Email: *haymiti02@gmail.com*
Authors: Sheleme Beyene, Email: *shelemeb@gmail.com;* Alemayehu Kiflu, Email: *alemanchy@gmail.com*

INTRODUCTION

Soil is a gradually renewable dynamic natural resource (Jenny, 2012) whose extents of proper utilization and effective management determine the sustainability of agricultural production (Adugna, 2016). Generally, soil is classified as natural body on the basis of its characteristics (Nikiforova et al., 2019), and soils in a given group are believed to be homogeneous (Tursina, 2012). Characterization of soils deals with the assessment of their morphological, physical, chemical, and mineralogical properties (Schaetzl and Thompson, 2015) while classification is the systematic categorization of soils into different groups at varying levels of generalization based on their overall properties (Ditzler, 2017; Buol et al., 2011). Besides, soil mapping is a process of creating a visual representation of the different soil types and their distribution within a specific geographic area (Wimalasiri et al., 2020; Kienast-Brown et al., 2017).

The action of characterization and classification is ultimate to all soil studies as it is a vital tool to reflect the real diversity of soils (Brevik et al., 2016; Buol et al., 2011). It also links research results and their beneficial extension with field applications (Ayalew et al., 2015) by providing key information about soil properties and environmental conditions (Lufega and Msanya, 2017). Hence, it helps in organizing of knowledge, ease of remembering of soil properties and understanding of relationships, having clear communication, and the best of technology transfer (Lufega and Msanya, 2017; Hartemink, 2015). According to Brevik et al.

(2016), characterization and classification of soils are done in the application of proper management practices, rehabilitation of degraded soils, and provision of a ready-made map legend for soil surveyors. Whereas, soil mapping aims to unravel deficiencies in our understanding of soil properties and processes both in time and space (Taha et al., 2019; Minasny and McBratney, 2016).

Toposequence is series of soils that vary primarily due to the topography as soil forming factor (Alves et al., 2024). This means each soil type in a toposequence exhibit distinctive characteristics that are directly related with the slope at typical components (crest, shoulder, back slope, foot slope, and toe slope) of a topography (Omokaro, 2023; Seifu and Elias, 2018). Moreover, topography is important in pedologic processes via determining the extent of water drainage and runoff, soil thickness and erosion potential, particle size distribution, reaction, and OM content (Omokaro, 2023; Begna, 2020). However, any patterns of soil association along a toposequence is not necessarily repeated with the topography in the landscape (Bonfatti et al., 2020; Ogban et al., 2019). Because soils with identical parent material, existing within a uniform climatic condition, and affected by similar soil-forming factors may still have varied characteristics due to local relief, internal drainage, and/or geomorphic attributes (Tunçay and Dengiz, 2020; Gruber et al., 2019). Hence, the concept of toposequence is a useful analytical tool in describing the outline of soil characterization, classification, and mapping for sustainable agricultural production and land use management (Seifu and Elias, 2018; Brevik et al., 2016).

Soil genesis and distribution in Ethiopia are influenced by agro-ecological zones accompanied by geology, topography, vegetation, and climatic variability (Weldegerima, 2024; Regassa et al., 2023). For instance, different soil units like Acrisols, Cambisols, Fluvisols, Leptosols, Luvisols, Nitisols, Vertisols, and Umbrisols with various qualifiers have been identified in the country (Ali et al., 2024; Tufa et al., 2021). The country has a long history of collecting basic information on soil characterization which is either limited to some selected potential areas or done with shallow observations and wider generalizations (Megarsa, 2023; Nyssen et al., 2019). Furthermore, the available soil maps in the country are dominantly small-scale and represent scattered areas which hinder site-specific soil interpretation and utilization (Seifu et al., 2023; Debele, 2018). Accordingly, detailed soil survey and mapping are imperative for better understanding and prediction of soil types and distribution at local physiographic variability level (Abdu et al., 2023; Megarsa, 2023; Fekadu et al., 2018).

Variation in the physiography of agricultural lands has an enormous influence on soil properties and plant production (Abdu et al., 2023; Laekemariam et al., 2016). Consequently, the absence of inclusive evidence on the nature of soils at the level of local variability is often a key factor limiting the development of Ethiopian agriculture (Seifu and Elias, 2018; Tamene et al., 2017), as it does particularly around the study area (Cherinet, 2017). Acquiring comprehensive soil information while doing an in-depth characterization and classification at local topographic condition or watershed level is important to make proper utilization and management of soils for sustaining food production, rehabilitating degraded land, and tackling site-specific soil related problems (Mathewos and Mesfin, 2024; Bedadi et al., 2023). Therefore, this study was conducted to characterize, classify, and map the soils along a toposequence of Qenberenaweti sub-watershed, Central highlands of Ethiopia.

MATERIALS AND METHODS

Description of the Study Area

The study was conducted in Qenberenaweti sub-watershed which is located between 09° 33′ 50″ and 09° 35′ 03″ N latitude and 39° 32′ 50″ and 39° 33′ 54″ E longitude (Figure 1). It is found at about 120 km northeast of Addis Ababa on the way to Debre Berhan and 18 km from the Chacha town of Angolelana Tera district, North Shewa zone of Amhara National Region State. The site covers a total area of 317 hectares on a plateau of the central Ethiopian highland system with elevations ranging between 2808 and 2960 meters above sea level (m.a.s.l).

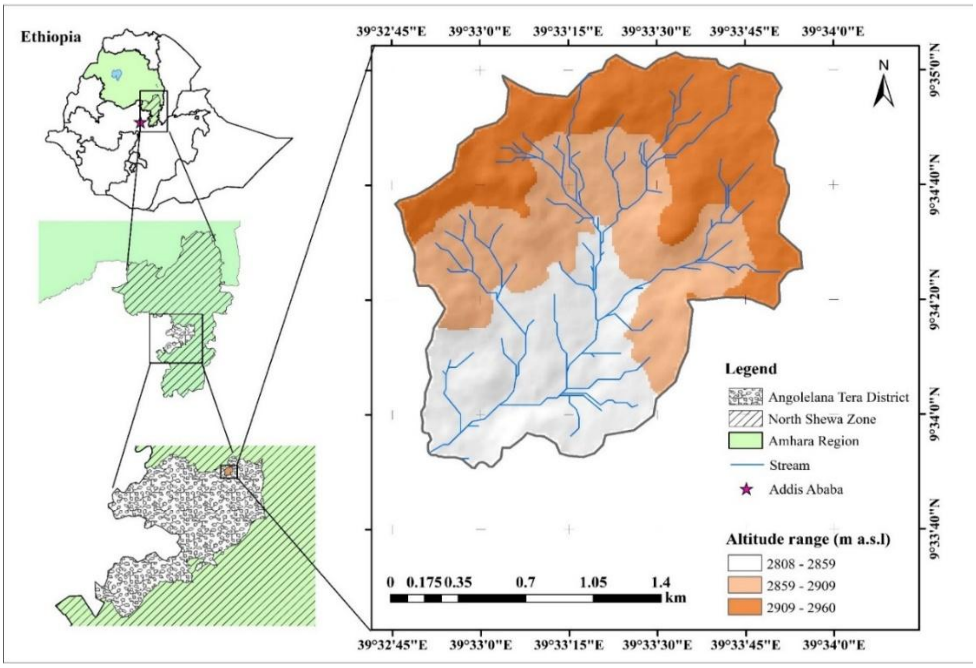

Figure 1. Location and altitude map of the study area

The rainfall distribution is bimodal, short (March to April) and long (June to September) rainy seasons, with mean annual precipitation of 928.5 mm. The mean annual temperature is 14.2 ℃ having monthly averages of 15.6 ℃ in May and 12.9 ℃ in October, respectively (Figure 2). Generally, the area falls under the Tepid to Cool Sub-Moist Mid-Highland agro-ecological zone (MoARD, 2005); and has Cambisols, Leptosols, and Vertisols as major soil types (ATDAO, 2017).

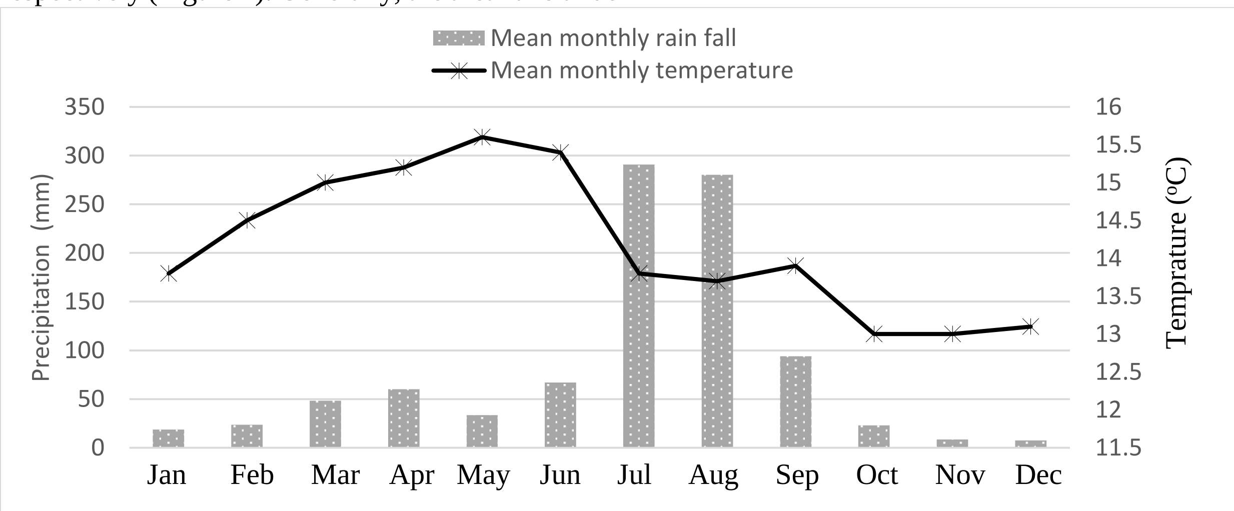

Figure 2. Mean monthly rainfall and temperature of the study area

Selection of Soil Sampling Sites and Identification of Mapping Units

Before the field survey, the topographic map (1:50,000) and areal image (Google Earth Pro) of the study area were interpreted to organize the vital site and land information: slope, altitude, drainage patterns, and land configurations. The overall topographic configuration and exact outlet point of the area were recognized during the field visit. Delineation of the sub-watershed and determination of its hydrological components were done using spatial analysis tools of Arc GIS 10.5 software after retrieving a 12.5 m digital elevation model (DEM) data from the United States Geological Survey (http://www.USGS.gov).

The free-soil survey (Driessen et al., 2000) method that followed a systematic sampling approach was employed across the north-south facing landscape configuration to identify the soil mapping units (SMU) with their boundaries. A given SMU was defined on the basis of similarity and/or closeness in key topographic and morphological (slope gradient, soil depth, and texture of surface soils) features of each augur sampling points. A total of 91 auger samples to 120 cm depth were collected using 'Edleman auger' unless limited by the stoniness or compactness of the soils. A toposequence along the major stream flow directions which have all the typical topographic components and represent the upper, middle, and lower positions was considered for excavation of a representative pit (1.5 m width by length and up to 2 m depth) and collection of peripheral surface soil samples. Coordinate points of all auger and profile inspections were taken by a handheld geographic positioning system (GPS) apparatus (Garmin-60) and digitized on the topographic map produced using Arc GIS 10.5 software.

Soil Sampling and Analysis

Both disturbed and undisturbed soils were sampled from every identified genetic horizon of the opened profiles. Additionally, twelve disturbed surface (0-20 cm) soil sub-samples were randomly collected within 15 m radius surrounding of each pedon. Then, the sub-samples were thoroughly mixed and made into three composites per pedon.

The disturbed soil samples were air-dried and ground to pass through a 2 mm sieve for analyses of most physicochemical properties except for the organic carbon (OC) and total nitrogen (TN) contents in which case soils were sieved by a 0.5 mm mesh size. The undisturbed samples were oven-dried at 105 ℃ for 24 hours to determine bulk density using the core-sampling method (BSI, 1975) while particle density with the pycnometer method (Tan, 1995). Soil particle size distribution was analyzed by the modified sedimentation hydrometer procedure (Bouyoucos, 1951).

The pH of the soils was determined in 1:2.5 soil-to-water suspension using a pH meter (Van Reeuwijk, 1995); and the suspension was also used to measure the EC of the soils with a conductivity meter. The organic carbon (OC) content was determined using the wet digestion method of Walkley and Black (Van Ranst et al., 1999). The total nitrogen (TN) content was analyzed by a wet-oxidation procedure of the Kjeldahl method (Bremner and Mulvany, 1982). The soil available phosphorus (Av. P) content was extracted following Olsen method (Van Reeuwijk, 1995) and the concentrations were measured using spectrophotometer at 882 nm. The exchangeable base cations (Ca, Mg, K and Na) and cation exchange capacity (CEC) of the soils were determined using 1M ammonium acetate (pH 7) method according to the percolation tube procedure (Van Reeuwijk, 1995). The concentrations of exchangeable Ca and Mg in the leachate were determined by Atomic Absorption Spectrophotometer (AAS); whereas the exchangeable K and Na contents were measured by a flame photometer. Available micronutrients (Fe, Mn, Zn, and Cu) were extracted using the diethylene-triamine-pentaacetic-acid (DTPA) method (Tan, 1995), and their concentrations were determined by AAS. The CEC due to the clay fraction (CEC clay) was computed by subtracting the CEC value of OM from CEC of soil (equation 1) with assumption of OC has a CEC of 200 cmolc kg-1 (Landon, 2014):

$$CECclay = \frac{CEC\ soil - (\%\ OM * 200)}{\%\ Clay} \quad \ldots\text{Equation1}$$

Description of the Pedons and Classification of the Soils

The in-situ description of soil properties was carried out following the guideline for soil profile description (FAO, 2006). Furthermore, the soils of the study area were classified according to the World Reference Base (WRB) for soil resources classification system (IUSS, 2022).

Statistical Analysis

The data on selected physicochemical properties of the surface soils were interpreted by descriptive statistics. Besides, Pearson's correlation matrix was used to explain the relationship pattern among all the variables. All statistical analyses were performed using the Statistical Package for Social Science (SPSS) software version 26.0 (IBM, 2020).

RESULTS AND DISCUSSION

Description of Soil Mapping Units and Site Characteristics

After the detailed in-situ detection of each soil augering point, 32 different soil mapping units (SMU) were identified in the sub-watershed (Figure 3). The upper topographic position occupied SMU-01, 02, 03, 04, 05, 06, 07, 08, 10, and 19 while the middle position had SMU-09, 11, 12, 15, 16, 17, 18, 20, 22, and 23. The rest (SMU-13, 14, 21, 24, 25, 26, 27, 28, 29, 30, 31, and 32) were found at the lower topographic position. A representative pit was dug on SMU-06, 05, 16, 17, 32, and 30 in lieu for the summit, shoulder, back slope, foot slope, toe slope, and bottom depression positions, respectively.

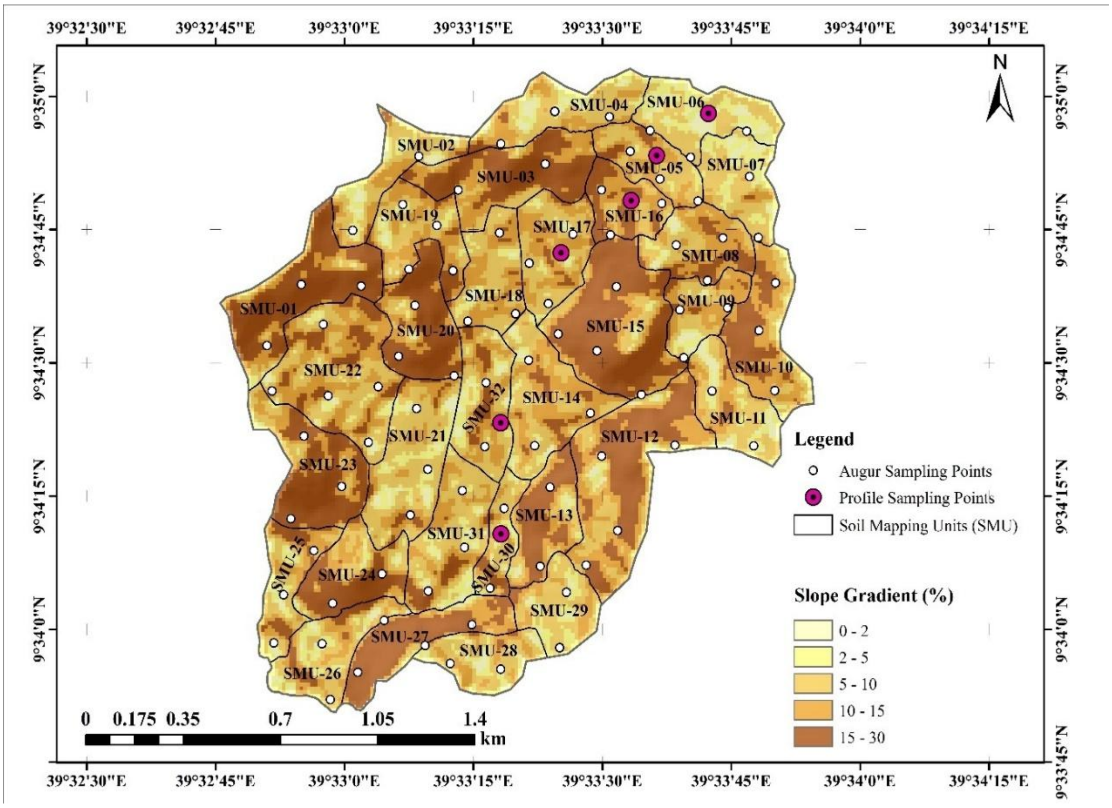

Figure 3. Topographic map of the study area

As shown in Appendix Table 1, the SMU-06, 07 and 30 were very deep soils (>120 cm) with clayey texture (feel method) at the surface of level (0-2 %) and gently level (2-5 %) lands. Amongst SMUs found on sloping lands (5-10 %), SMU-04, 21, 28, 31, and 32 had very deep profiles while SMU-02, 18, 26, and 29 were categorized as deep soil (100-120 cm). The soils of SMU-02, 04, 18, 26, 29, 31, and 32 were clayey while that of SMU-21 and 28 were clay loam in texture. The strongly sloping land (10-15 %) was occupied by SMU-05, 14, 17, 22 and 25 with soils having deep solum and clay loam texture. They were also partly covered by very deep SMU-11 and 19 and deep SMU-08 and 09 solum with clay textured soils at the surface. Although many of the SMUs (01, 03, 10, 15, 20, 23, 24, and 27) existing on moderately steep slope land (15-30 %) had a moderately deep (50-100 cm) solum with clay loam textured surface soils, the few (SMU-12, 13, and 16) were deep soils with a clay texture.

The variations in the depth of the solum and soil texture at the surface might be related to the shape and length of the slope which determine the degree of soil material translocation and accumulation via the action of water flowing down the slope. Depth of the solum and soil texture at the surface are ascribed to slope features (Mwendwa, 2021; Subhatu et al., 2018) that erode, move, and depose finer soil materials via the action of the running water from upper to bottom topographic positions (Debele et al., 2018). Consequently, the nature of slope in a given landscape can influence the rate of soil formation and development at different topographic positions (Deressa et al., 2018; Mulugeta and Sheleme, 2010). All the pedons were opened on grazing and fallow land uses that had distinctive parent materials of basaltic igneous rock (Table 1). The pedons have existed on different landforms and slope gradients with straight slope forms and straight plus concave surface flow pathways. Rill and sheet soil erosions were observed at shoulder, back-slope, and foot-slope positions, whereas soil deposition was prevalent on the toe-slope and bottom depression areas. Also, the surface of the eroded topographic components was covered by different amounts and sizes of coarse fragments. However, there was no rock outcrop and sign of surface sealing in the area. The data gathered from auger inspection and site characteristics of the study area revealed the presence of variations in key topographic features that determine the nature (morphological, physical, and chemical properties) and distribution of soils along the toposequence.

Table 1. Selected site characteristics of pedons along the toposequence

Basic information	Profiles: Summit	Shoulder	Back-slope	Foot-slope	Toe-slope	Depression
Coordinates (Latitude/Longitude)	09°34'58''N 39°33'42''E	09°34'53''N 39°33'36''E	09°34'48''N 39°33'33''E	09°34'42''N 39°33'25''E	09°34'23''N 39°33'18''E	09°34'11''N 39°33'18''E
Altitude (masl)	2957	2946	2927	2894	2859	2845
Major landform	Level land, plain	Sloping land, medium-gradient escarpment	Sloping land, medium-gradient hill	Sloping land, dissected plain	Level land, depression	Level land, depression
Slope gradient (%)	Level (0.5)	Strongly sloping (10)	Moderately steep (17)	Strongly sloping (12)	Sloping (5)	Gently sloping (2)
Slope form and surface flow pathway	Straight-Straight	Straight-Concave	Straight-Concave	Straight-Straight	Straight-Straight	Straight-Straight
Land use	Grazing	Fallowing	Fallowing	Fallowing	Grazing	Grazing
Geologic materials	Basic Igneous rock (Basalt)	Basic Igneous rock (Basalt)	Basic Igneous rock (Basalt)	Basic Igneous rock (Basalt)	Basic Igneous rock (Basalt)	Basic Igneous rock (Basalt)
Parent materials	Weathered products of rocks with a high amount of a 2:1 expanding clay type (smectite)	Saprolite	Saprolite	Variety of fine to medium textured unconsolidated materials from alluvial and colluvial deposits	Fine-textured materials (clay and silt fractions) derived from alluvial deposit	Fine-textured materials (clay and silt fractions) derived from alluvial deposit
Rock outcrops	None	None	None	None	None	None
Surface cover (%) and size dimension (cm) of coarse fragments	None	Many (15-40) stones (6-20)	Common (5-15) boulders (20-60)	Few (2-5) stones (6-20)	None	None
Category, affected area (%), and degree of erosion or material deposition	No evidence	Rill erosion, 10-25, moderate	Rill erosion, 10-25, moderate	Sheet erosion, 5-10, slight	Deposition by water	Deposition by water
Surface sealings	None	None	None	None	None	None
Width (cm), depth (cm) and distance between (m) surface cracks	Very wide (5-10), very deep (>20) and moderately wide spaced (0.5-2)	Wide (2-5), very deep (>20) and widely spaced (2-5)	None	Medium (<1), medium (2-10) and widely spaced (2-5)	None	None
Soil type (WRB)	Vertisol	Cambisol	Leptosol	Luvisol	Cambisol	Cambisol
Local soil name	*Merere*	*Areda*	*Ajara*	*Bodda*	*Abolsie*	*Abolsie*

Soil Morphological Properties

The pedons had A and B sequence of horizons with their depth varying from 135 to 200+ cm (Table 2). In general, the thickness of A-horizons showed an increasing trend down the slope with the exception of the horizon at the back-slope. The shallowest (20 cm) and deepest (70 cm) A horizons existed at the back slope and toe slope, respectively (Table 2). The disparity in surface horizon thickness might be attributed to slope steepness and form at a particular topographic position which determine soil formation and development by influencing horizontal (erosion and deposition) and vertical (eluviation and illuviation) translocations of soil material. An increase in the depth of surface horizon along toposequences largely occurs due to water erosion that takes soil materials from summit to bottom depression (Sheleme, 2017; Alemayehu et al., 2016; Dessalegn et al., 2014). The relatively gentler slope at the lower topographic locations aids the deposition of materials eroded from the upper part (Chaplot, 2013; Ali et al., 2010). In line with the present findings, (Mulugeta and Sheleme, 2010) also found a reduction in the depth of surface soils with increasing slope along the toposequences of Kindo Koye sub-watershed in southern Ethiopia, whereby the thinner and thicker A-horizons appeared at the steep (shoulder and back) and gentle (foot and toe) slopes, respectively.

The distinctness and topography of horizon boundaries between the surface and sub-surface horizons were abrupt and smooth, except for the clear-wavy and abrupt-wavy boundaries for the pedons at the summit and bottom depression areas (Table 2). The variations in the appearance of horizon boundaries indicate that the soils were formed through different soil-forming processes (Ayalew et al., 2015) while they partly reflect anthropogenic impacts (Cools and De Vos, 2010). The boundary changes between surface and sub-surface horizons of cultivated land-use occurred because of repeated human activities like plowing (Hailu et al., 2015). Moreover, the changes in grazing land use could be due to gradual transformation, homogenization, and/or erosional-depositional processes (Ande, 2010). The color of the surface soils was very dark brown (7.5YR 2.5/2 or /3) at the upper while it was dark reddish brown at the middle (5YR 3/3) and lower (5YR 2.5/2) slope positions (Table 2). The surface soil colors of the pedons were darker than their subsurface counterparts except for the pedons at the summit and shoulder (Table 2). The color variations within and among the pedons might be the reflection of differences in chemical and mineralogical composition, topographic positions, OM content, and moisture regimes. (Dengiz et al., 2012) confirmed that soil color was related to OM and carbonate accumulations, redoximorphic features, drainage condition, and physiographic position. Similarly, several authors reported that the surface horizons have darker colors than the corresponding subsurface horizons as a result of relatively higher soil OM contents in the surface layers (Dessalegn et al., 2014; Ali et al., 2010; Mulugeta and Sheleme, 2010). Mulugeta and Sheleme (2010) also reported that soils on slopes that have never been saturated with water had reddish and brownish subsoil colors while soils on poorly drained locations tended to have grey-colored B-horizons. However, the greyish subsurface soils color at the summit could be due to the limited weathering of smectite clays that remain stable as long as the pH is above neutral and result in subsoils with a lower red hue and weaker chroma because of the less free ferric ions (Driessen et al., 2001). Besides, the blackish/greyish sub-surfaces at the shoulder could be due to the leaching accumulation of weathered smectitic clays that impede internal drainage upon cementation of subsoil particles while providing reddish soil color owing to Fe^{3+} compounds left behind in the surface horizon (Driessen et al., 2001).

The structures of soils at the surface layers were granular and sub-angular blocky with grades ranging from moderate and moderate to strong and fine to coarse sizes (Table 2). On the other hand, the subsurface horizons had different structures (angular blocky, sub-angular blocky, prismatic, columnar, platy, and crumbly) weak to moderate and strong grades, and fine to very coarse sizes. The presence of granular structure at the surface could be attributed to the OM content (Gebrekidan and Negassa, 2006), whereas the well-developed structure in the subsurface is due to increasing clay content (Khormali et al., 2003). The results corroborate with Fekadu et al. (2018); Mesfin et al. (2017); Teshome et al. (2016) who found granular soil structure in the surface horizons that changed to angular and sub-angular structures in the sub-surface horizons of the pedons.

Table 2. Morphological properties of soils along the toposequence of Qenberenaweti sub-watershed

Profile	Horizon	Depth (cm)	Boundary	Soil Color (Munsell Code) Dry	Soil Color (Munsell Code) Moist	Soil Structure (Grade/ Size/ Shape)	Soil Consistency Dry	Soil Consistency Moist	Wet Plasticity	Wet Stickiness	Texture (Feel)
Summit	A	0-25	CW	10YR 3/3	7.5YR 2.5/2	Mo/ Me/ Gr	HA	VFR	PL	VST	Clay
	Bt1	25-70	AS	10YR 4/1	7.5YR 3/1	St/ Co/ Ab	VHA	FI	VPL	VST	Clay
	Bt2	70-105	CW	10YR 4/2	10YR 3/2	St/ Co/ Pr	EHA	FI	VPL	VST	Clay
	Btk1	105-135	AS	10YR 4/3	7.5YR 3/3	MS/ Co/ Ab	VHA	VFI	PL	VST	Clay
	Btk2	135-165	AW	10YR 4/3	7.5YR 3/2	MS/ Me/ Sb	HA	FI	VPL	ST	Clay
	Btkm	165-200	-	10YR 4/4	7.5YR 4/2	MS/ Me/ Cr	HA	FR	PL	ST	Clay
Shoulder	A	0-30	AS	10YR 3/4	7.5YR 2.5/3	MS/ Me/ Gr	SHA	VFR	VPL	ST	Clay loam
	AB	30-65	CS	10YR 3/3	7.5YR 2.5/2	Mo/ Fi/ Cr	SHA	VFR	VPL	VST	Clay loam
	Bt1	65-100	AW	10YR 3/1	7.5YR 2.5/1	St/ Me/ Pr	VHA	FR	VPL	VST	Clay
	Bt2	100-120	GW	10YR 4/1	7.5YR 3/1	St/ Me/ Pl	HA	VFI	VPL	VST	Clay
	BC	120-135	-	10YR 4/2	7.5YR 3/2	MS/ Fi/ Cr	SHA	FR	PL	ST	Clay loam
Back slope	Ac1	0-20	AS	7.5YR 3/3	5YR 3/3	Mo/ Me/ Sb	SHA	VFR	PL	ST	Loam
	Ac2	20-40	CW	7.5YR 3/4	5YR 3/3	Mo/ Me/ Sb	HA	FR	PL	ST	Loam
	Bwv	40-60	CS	7.5YR 3/2	5YR 3/2	MS/ Me/ Sb	VHA	FI	PL	ST	Clay loam
	Bhsm	60-110	CW	7.5YR 3/2	7.5YR 2.5/2	St/ Me/ Ab	VHA	VFI	VPL	VST	Clay loam
	Btx	110-125	AW	7.5YR 4/4	7.5YR 3/3	MS/ Me/ Cr	HA	FI	VPL	VST	Clay loam
	B/C	125-155	-	7.5YR 4/3	7.5YR 3/3	St/ Me/ Cr	HA	FR	PL	ST	Clay loam
Foot slope	Ac1	0-35	AS	7.5YR 3/4	5YR 3/3	Mo/ Co/ Sb	SHA	VFR	PL	ST	Clay loam
	ABc2	35-70	CS	7.5YR 3/2	5YR 3/2	Mo/ Me/ Sb	HA	FR	PL	ST	Clay
	Btc3	70-95	CW	7.5YR 3/3	7.5YR 2.5/2	Mo/ Me/ Ab	HA	FR	PL	VST	Clay
	2Bti1	95-150	AS	10YR 3/1	7.5YR 2.5/1	St/ VC/ Cl	SHA	VFR	VPL	VST	Clay
	2Bti2	150-200+	-	10YR 2/1	7.5YR 2.5/1	St/ Co/ Cl	VHA	FI	VPL	VST	Clay
Toe slope	Ac1	0-20	AS	7.5YR 3/3	5YR 2.5/2	Mo/ Me/ Gr	SHA	VFR	PL	ST	Clay loam
	Ac2	20-45	AS	7.5YR 3/4	5YR 3/2	Mo/ Fi/ Gr	SHA	FR	PL	ST	Clay loam
	Ac3	45-70	CS	7.5YR 4/4	5YR 3/2	Mo/ Fi/ Cr	HA	FI	VPL	ST	Clay
	Bhc4	70-105	CW	7.5YR 3/2	7.5YR 2.5/2	Mo/ Me/ Cr	HA	VFI	VPL	VST	Clay
	B/C	105-165+	-	7.5YR 4/2	5YR 2.5/2	WM/ Me/ Cr	HA	FR	PL	ST	Clay loam
Bottom depression	Ag1	0-30	AW	7.5YR 3/4	5YR 2.5/2	Mo/ Fi/ Gr	HA	FR	VPL	ST	Clay loam
	Aqg2	30-65	GW	7.5YR 3/3	5YR 3/2	Mo/ Me/ Sb	SHA	VFR	VPL	VST	Clay loam
	Bg3	65-110	CW	7.5YR 3/3	5YR 3/2	Mo/ Me/ Ab	HA	FR	VPL	ST	Clay
	Bhg4	110-140	CW	7.5YR 3/2	5YR 3/2	Mo/ Fi/ Ab	SHA	FR	VPL	VST	Clay
	BCg5	140-190	-	7.5YR 4/3	7.5YR 2.5/2	WM/ Fi/ Cr	HA	FR	PL	ST	Clay loam

Where: AS-Abrupt Smooth; CS-Clear Smooth; AW-Abrupt Wavy; CW-Clear Wavy; GW- Gradual Wavy; St-strong; Mo-moderate; We-weak; MS-moderate to strong; WM-weak to moderate; VC-very coarse; Co-coarse; Me-medium; Fi-fine; Cr-crumbly; Ab-angular blocky; Sb-subangular blocky; Gr-granular; Pr-prismatic; Cl-columnar; Pl-platy; HA-hard; VHA-very hard; SHA-Slightly hard; FI-firm; FR-friable; VFR-very friable; PL-plastic; VPL-very plastic; ST-sticky; VST-very sticky

The soils along the toposequence had consistence ranging from hard to slightly hard, friable to very friable, and plastic/sticky to very plastic/very sticky at the surface horizons while the soil consistence in the subsurface horizons varied from hard to extremely hard, very friable to firm and plastic/sticky to very plastic/very sticky (Table 2). The variations in soil consistence could be resulted from the differences in particle size distribution, texture, OM content, and amount and nature of clay particles (Paltseva, 2024; Ayalew et al., 2015; Moradi, 2013). Very friable and friable consistencies were observed in the surface soils as a result of higher OM contents compared to their subsurface counterparts (Debele et al., 2018; Mulugeta and Sheleme, 2010) and impacted better workability of clayey soils by reducing their stickiness (Ali et al., 2010). In contrast, sticky/very sticky and plastic/very plastic consistencies show the existence of high clay and low organic carbon contents with difficulty to till (Ayalew et al., 2015). Furthermore, (Ali et al., 2010) pointed out that very sticky and very plastic appearances could be best indicative of the presence of smectitic clays in the soils.

Soil Physical Properties

The textural class of all soils at the surface and subsurface horizons was clay with different distribution of the three soil separates (Table 3). The proportion of the separates is determined by slope steepness, form, and topographic laying position of the excavated pedons (Ofori et al., 2013). The sand fraction in the surface layer increased from 18% at the summit to 32% at the back-slope, and then decreased to 24% at the bottom depression position, whereas the clay decreased from 48% to 40%, and then increased to 48% at the respective topographic positions (Table 3). The coarser soil texture in the surface horizons at the middle part of the toposequences might be due to the selective removal of fine (clay) and medium (silt) sized soil particles by the action of erosion from steeper slope at this topographic position and their deposition at lower parts. It is likely that silt proportion would be raised on foot and toe slopes as compared to the surface soils on the shoulder and back slopes when erosion left coarse particles on the hill part (Mulugeta and Sheleme, 2010). The highest amount of clay particles at the surface of the bottom depression position could be attributed to their translocation and deposition from the upper and adjacent profiles (Babalola et al., 2007).

On the other hand, the subsurface horizons of most pedons were finer in texture than their respective surface horizons due to the downward translocation of clay particles (Table 3). The presence of clay illuviation is the main factor in the formation of the argillic horizon in the subsurface soils of the upper and middle slope profiles (Mulugeta and Sheleme, 2010). In line with this finding, Adhanom and Toshome (2016); Mulugeta and Sheleme (2010) found an increasing trend of clay contents while sands showed a decreasing trend down the slope gradient due to selective movement of finer soil particles laterally from the upper slopes and/or adjacent areas and subsequent accumulation in the lower topographic position. Accordingly, the higher clay content in the B horizon of soils was reported as a result of illuviation, predominant *in-situ* pedogenetic formation in the subsoil, destruction in the surface horizon, upward movement of coarser particles due to swelling and shrinking, biological activity, and a combination of two or more of these different processes (Fekadu et al., 2018; Yitbarek et al., 2018; Mesfin et al., 2017). The very high significant ($P \leq 0.01$) correlations between clay and sand ($r = -0.82$) and silt ($r = -0.80$) also confirm the translocation and illuvial accumulation of clay in the subsurface horizons (Appendix Table 2).

The silt to clay ratio of the soils across the profiles ranged from 0.19 to 1.00 (Table 3); hence, implying that the soils are at a relatively better rate of weathering with significant leaching of clay particles. Soils having silt to clay ratio below a unity are considered to be at an advanced stage of development and had undergone feralitic pedogenesis process (Debele et al., 2018; Abayneh, 2005). The lower silt to clay ratios in the subsoil layers as compared to their surface counterparts also confirm the existence of clay migration in the pedons (Nahusenay et al., 2014; Beyene, 2011). The presence of an appreciable amount of silt fraction in the surface soils could increase the water-absorbing ability of the soils, and facilitate longer soil-water retention for plant use (Saha et al., 2020; Beyene, 2011)

Table 3. Physical properties of soils along the toposequence of Qenberenaweti sub-watershed

Profile	Horizon	Depth (cm)	Particle Size (%)			Silt to Clay Ratio	Textural Class	Density (g cm^{-1})		Total Porosity (%)
			Sand	Silt	Clay			Bulk	Particle	
Summit	A	0-25	18	34	48	0.71	Clay	1.22	2.35	47.97
	Bt1	25-70	14	14	72	0.19	Clay	1.24	2.39	48.33
	Bt2	70-105	12	14	74	0.19	Clay	1.30	2.43	46.50
	Btk1	105-135	18	14	68	0.21	Clay	1.35	2.42	44.10
	Btk2	135-165	14	24	62	0.39	Clay	1.29	2.51	48.50
	Btkm	165-200	10	18	72	0.25	Clay	1.41	2.56	45.12
Shoulder	A	0-30	26	28	46	0.61	Clay	1.19	2.43	51.03
	AB	30-65	22	26	52	0.50	Clay	1.21	2.42	50.00
	Bt1	65-100	18	16	66	0.24	Clay	1.29	2.50	48.30
	Bt2	100-120	12	16	72	0.22	Clay	1.40	2.58	45.63
	BC	120-135	26	22	52	0.42	Clay	1.31	2.56	48.73
Back slope	Ac1	0-20	32	28	40	0.70	Clay	1.19	2.41	50.62
	Ac2	20-40	28	28	44	0.64	Clay	1.23	2.44	49.59
	Bwv	40-60	30	24	46	0.52	Clay	1.28	2.56	49.90
	Bhsm	60-110	20	34	46	0.74	Clay	1.30	2.53	48.62
	Btx	110-125	18	20	62	0.32	Clay	1.29	2.47	47.87
	B/C	125-155	24	28	48	0.58	Clay	1.40	2.57	45.72
Foot slope	Ac1	0-35	30	28	42	0.67	Clay	1.19	2.35	49.36
	ABc2	35-70	24	38	38	1.00	Clay Loam	1.16	2.39	51.67
	Btc3	70-95	18	26	56	0.43	Clay	1.26	2.49	49.40
	2Bti1	95-150	14	16	70	0.23	Clay	1.36	2.64	48.39
	2Bti2	150-200+	14	16	70	0.23	Clay	1.42	2.60	45.58
Toe slope	Ac1	0-20	26	32	42	0.76	Clay	1.15	2.37	51.37
	Ac2	20-45	26	30	44	0.68	Clay	1.20	2.43	50.82
	Ac3	45-70	24	32	44	0.73	Clay	1.19	2.41	50.62
	Bhc4	70-105	22	28	50	0.56	Clay	1.24	2.48	50.10
	B/C	105-165+	36	18	46	0.39	Clay	1.28	2.61	50.96
Bottom depression	Ag1	0-30	24	28	48	0.58	Clay	1.18	2.43	51.34
	Aqg2	30-65	34	16	50	0.32	Clay	1.20	2.50	51.90
	Bg3	65-110	20	26	54	0.48	Clay	1.19	2.45	51.33
	Bhg4	110-140	20	28	52	0.54	Clay	1.23	2.59	52.51
	BCg5	140-190	34	20	46	0.43	Clay	1.29	2.55	49.31

The bulk and particle densities of the surface horizons ranged from 1.15 to 1.22 and 2.35 to 2.43 g cm^{-3}, respectively, whereas their corresponding values in the subsurface horizons ranged from 1.16 to 1.42 and 2.39 to 2.64 g cm^{-3} (Table 3). The bulk density values of the soils in the surface horizons were under the usual ranges (1.0-1.5 g cm^{-3}) for fine-textured soils (Wogi et al., 2021). Both the particle and bulk densities of the soils increased with soil depth at all topographic positions which could be due to the relatively higher OM content in the surface than the subsurface soils; while the increase in bulk density could also result from natural compaction of the subsurface soils by a load of surface soils (Abayneh, 2005). According to Mulugeta and Sheleme (2010), soils that are loose, porous, or well-aggregated may have lower bulk densities than soils that are compacted or non-aggregated.

The total pore space in the surface layers was between 47.97 and 51.37% showing a decreasing trend with soil depth (Table 3). According to Michael (2009), the total pore spaces in the clayey textured soils may vary between 40 and 60 %. Besides, Shahab et al. (2013) also stated that the optimum total pore space value for crop production is about 50 %. Hence, the studied soils could be considered convenient for better crop production as there is a conducive situation for free aeration and water movement within the soil structure that is also capable of determining the number, diversity, and activity of important soil organisms (Mulugeta et al., 2019).

Table 4. Mean values of particle-size distribution of the soils around excavated pedons

	Percent sand			Percent silt			Percent clay			Textural
Pedon	Mean	SD	CV (%)	Mean	SD	CV (%)	Mean	SD	CV (%)	**class**
Summit	19	1	5.26	33	1	3.03	49	1	2.04	Clay
Shoulder	23	3	13.04	29	1	3.45	49	3	6.12	Clay
Back-slope	30	2	6.67	31	3	9.68	39	1	2.57	Clay loam
Foot-slope	28	2	7.14	31	2	6.45	41	1	2.40	Clay
Toe-slope	27	1	3.71	29	1	3.45	43	1	2.33	Clay
Bottom depression	25	1	0.04	29	1	3.45	46	2	4.35	Clay

The surface soil samples collected from all directions of the opened pedon had more or less similar texture with that of the corresponding soils of the surface horizons, except for a slight difference at the back-slope pedon. However, the proportion of clay, silt, and sand fractions at a given physiographic position deviated by ±1 to 3 % between the soils of the surface horizons of the pedons and the respective surface soils around the pedons (Table 4). In general, the descriptive statistics analysis reviled the presence of very closeness (CV < 15 %) within each of the three soil separates of the samples around the opened pedons (Wilding and Drees, 1978).

Soil Chemical Properties

The pH values of surface and sub-surface soils ranged from 5.59 to 6.23 and from 5.31 to 7.65, respectively (Table 5). According to Wogi et al. (2021), the surface soils at the shoulder and toe slope parts were slightly acidic while the others were moderately acidic. Apart from the toe slope, the pH values in the subsurface horizons were higher than the surface horizons of the rest pedons (Table 5). The escalations in pH values in the subsoils could be due to the illuvial accumulation of basic cations i.e., leaching and downward translocation of basic cations (Fekadu et al., 2018; Nahusenay et al., 2014). Additionally, it might be due to less H^+ released from the poor decomposition of the lower OM content in the subsoils (Ayalew and Beyene, 2012). The higher pH at the surface of the toe-slope position could also be related to the effects of water moving down the slope of the toposequence causing erosion and deposition of materials rich in basic cations. Generally, the low topographic positions had higher pH values than the upper positions, which might be due to the excessive accumulation of exchangeable bases that were laterally removed from uphills and subsequently deposited at lower slopes (Hailu et al., 2015; Nahusenay et al., 2014). However, the high pH value at the surface of the shoulder site could be associated with the substantial deposition of dust particles that blown-up from the nearby main paved road of magnesitic ($MgCO_3$), dolomitic [$CaMg(CO_3)_2$], and/or serpentine [$Mg_3Si_2O_5(OH)_4$] limestone sources.

On the other hand, the lower pH values at the sub-surface horizon of the toe-slope could probably be due to infiltration and percolation of water deep into the soil. The soil water saturation might have removed basic cations from the subsoil horizon and contributed to the lowering of soil pH (Damene et al., 2007). In addition to the release of H^+ from its numerous acid functional groups, OM facilitates leaching loss of Ca^{2+} and Mg^{2+} by forming soluble complexes (Jalali and Arfania, 2010; Brady and Weil, 2008). This finding agreed with the work of Fekadu et al. (2018) and Ali et al. (2010) whereby the pH-H_2O showed a general rise with soil depth in the pedons at upper and middle slope positions compared to those at the bottom and toe slope positions. The correlation analysis also revealed that the soil pH was caused negatively due to the OC ($r = -0.45$, $P \leq 0.01$), av. Fe ($r = -0.69$, $P \leq 0.001$) and av. Mn ($r = -0.50$, $P \leq 0.01$) contents while positively from the ex. Na ($r = 0.71$, $P \leq 0.001$), ex. K ($r = 0.39$, $P \leq 0.05$) and ex. Ca ($r = 0.39$, $P \leq 0.05$) concentrations (Appendix Table 2).

Irrespective of the topographic positions, the surface horizons of all pedons had relatively low soil electrical conductivity (EC) values (0.087 to 0.273 dS m^{-1}). The soils of the study area were non-saline (Havlin et al., 2017; Richards et al., 1954) with a very low rated EC value (Shaw, 1999) at which the existing amounts of soluble salts cannot affect the growth and productivity of most crops (Landon, 2014; Richards et al., 1954).

The organic carbon (OC) and total nitrogen (TN) contents across the horizons varied from 0.22 to 2.03% and from 0.02 to 0.18%, respectively (Table 5) while the carbon to nitrogen (C: N) ratio was between 6.0 and 20.0. In general, the OC and TN contents decreased with the soil depth, except for a substantial accumulation of illuviated OM in some subsurface horizons of the back slope and bottom depression parts. Additionally, the OC and TN contents of surface soils declined from the summit to the back slope, increased at the foot slope and toe slope, and then decreased at the bottom depression (Table 5). The surface soils were rated as medium (1.5-3.0 %) in OC and high (0.12-0.25 %) in TN contents (Wogi et al., 2021), whereby their C: N ratio falls under the low (10-15) category (Newey, 2006). According to (Hartz, 2007), soils with less than 0.07 % TN are believed to have a limited N mineralization potential while those having above 0.15 % are expected to mineralize a significant amount of N during the next crop cycle, showing that most of the studied soils have a good potential of N mineralization. In most cases, the C: N ratios of soils were within the common range (8:1 to 15:1) for arable soils (Brady and Weil, 2008) implying that OM was fully decomposed and N loss was apprehended.

The variations in OC and TN contents might be due to repeated tillage with poor management practices including complete removal of crop residues and/or reduced usage of organic amendments (Sheleme, 2023). The low content of OC in the surface layers could be attributed to the rapid decomposition and mineralization of OM under cultivation practices (Beyene, 2011; Dengiz, 2010) and then resulting in a reduction of TN (Adhanom and Toshome, 2016). The relatively better level of OC in the surface horizon of the summit, toe-slope and bottom depression parts might have been due to biomass turnover of grasses on the grazing land use (Fekadu et al., 2018). The similar distribution pattern of OC and TN with soil depth was also evident from the positive ($r = 0.93$) and very highly significant ($P \leq 0.001$) correlation between the two parameters (Appendix Table 2).

The available P (av. P) concentrations in surface soils ranged from 8.43 to 23.96 mg kg^{-1}, while they ranged from 0.48 to 24.27 mg kg^{-1} in the subsurface soils (Table 5). According to Wogi et al. (2021), the surface soils had low to high av. P contents while the subsoils were under very low to high ranges. The content of av. P was increased from the surface to the immediate subsurface horizon and declined with depth then after except for the pedon at the toe-slope probably due to leaching accumulation. Though its availability is determined by the P adsorption capacity (Deressa et al., 2018), soils with a near-neutral pH have the highest av. P than those under acidic reaction (Yitbarek et al., 2018; Beyene, 2011). The extent of microbially mediated P mineralization and immobilization processes could also determine its availability to plants (Zhu et al., 2018). Generally, there were variations in the availability of P along the toposequence with an alternative decrease-increase trend from the summit to bottom depression perhaps due to differences in the soil types, topography, level of inherent P content, use of P-containing fertilizers, and soil management practice in the area (Debele et al., 2018; Mulugeta and Sheleme, 2010). The lowest av. P in the surface soil of the bottom depression could be evidence of the soils with Fe mottling and concretions had low labile P fraction (Deressa et al., 2018) which become less available because of its bound to oxides of Fe and Al (Gérard, 2016).

Similar to this finding, different scholars confirmed that the av. P content decreases with increasing soil depth because of a decline in soil OM and/or a rise in clay contents (Yitbarek et al., 2018; Nahusenay et al., 2014; Mulugeta and Sheleme, 2010). Besides, Deressa et al. (2018) reported differential P distribution along a toposequence in mountainous topography and undulating landforms of humid western Ethiopia due to lateral and vertical movements of soil materials via the action of water. Mulugeta and Sheleme (2010) found a general increase in the distribution of av. P down the slope because of the strong association between slope position and soil properties. This was also confirmed by the positive correlations of av. P with OC ($r = 0.42$, $P \leq 0.05$), av. Fe ($r = 0.54$, $P \leq 0.01$) and av. Mn ($r = 0.44$, $P \leq 0.001$) contents, whereas it was negatively correlated with pH ($r = -0.42$, $P \leq 0.05$) and clay ($r = -0.51$, $P \leq 0.01$) content (Appendix Table 2).

The amounts of exchangeable Ca, Mg, K, and Na ranged from 10.80 to 32.26, 2.86 to 26.84 0.36 to 0.92, and 0.14 to 0.37 $cmol_c$ kg^{-1} (Table 5) that were under high to very high, medium to very high, medium to high, and low to medium ranges, respectively (Wogi et al., 2021). All the cations had an irregular pattern across the soil depth; but both the divalent cations showed systematic trends of increase-decrease along the toposequence. Moreover, Ca was the abundant cation on exchange sites which accordingly followed by Mg, K, and Na except for the Mg dominance over Ca at the surface layer of the back slope and depression pedons. The cationic swarming of soil colloidal surface often reported as $Ca^{2+} > Mg^{2+} > K^{+} > Na^{+}$ (Fekadu et al., 2018; Yitbarek et al., 2018; Adhanom and Toshome, 2016); and thought as an ideal for normal plant growth and development (Havlin et al., 2017).

Apart from the soils in the summit position, the surface soils of all pedons had Ca: Mg ratios below the approximate optimum (3:1 to 4:1) range for most crops to face a Mg-induced Ca deficiency (Landon, 2014). Besides, the Ca: Mg ratios of the surface soils at the back slope and bottom depression positions were below the suggested lowest acceptable (1:1) limit, whereby Ca availability is curtained (Landon, 2014). The existing variabilities in amount and distribution of the basic cations could be attributed to differences in the soil type (parent material), stage of weathering and development, erosion and deposition, translocation and leaching, and mining by cropping systems (Hailu et al., 2015; Nahusenay et al., 2014; Ali et al., 2010). In addition to the presence Mg bearing minerals, the dominance of Mg over Ca could be ascribed to its primal release after a relatively more weathering; strong adsorption at lower pH; and better occluding into clay minerals for smaller atomic size (Tardif et al., 2019; Senbayram et al., 2015; Gransee and Führs, 2013).

The overall cation exchange capacity (CEC) of soils in the study area ranged between 29.07 and 48.84 cmolc kg^{-1} (Table 5), which is under high and very high categories (Wogi et al., 2021). The CEC of surface horizons varied inconsistently along the toposequence whereby the highest CEC value was obtained from the bottom depression part followed by the foot slope, summit, back slope, shoulder, and toe slope positions. Though the CEC of the soils did not show any regular pattern with soil depth, higher CEC values were recorded in the subsurface horizons of the pedons than their surface counterparts.

The varying values of CEC down the soil depth and topographic positions could be linked with soil OC and clay contents (Debele et al., 2018). The highest CEC in the bottom layers of pedons at the lower (bottom depression) and middle (foot slope) topographic positions could be the result of the higher clay accumulation, whilst the lowest CEC at the surface layers of the pedon at the upper (shoulder) topographic position could be due to lateral and/or vertical movements of clay particles (Deekor et al., 2012; Nega and Heluf, 2009). In line with the present findings, Abate and Kibret (2016) found higher CEC in subsurface layers as compared to the surface layers in pedons at different topographic positions.

With respect to the decreasing trend of CEC along the slope, (Debele et al., 2018) also reported that pedons at upper and middle slope positions relatively had higher CEC than the lower part. The CEC had a highly significant positive relation with clay ($r = 0.46$) and pH ($r = 0.48$) while its correlation with OC ($r = -0.21$) was non-significant and negative (Appendix Table 2). The non-significant correlation of CEC with OM as compared to the highly significant with clay implies that the release of permanent (pH-independent) charges due to the isomorphous substitution of cations on clay minerals of the study soils contributed to the CEC than OM (Van Ranst, 2006).

The CEC clay varied between 52.23 and 99.47 cmolc kg^{-1} whereby higher results were recorded on subsurface horizons of all pedons except for the surface horizons at summit and shoulder. Moreover, the values increased from summit to foot slope; then failed and rose at toe slope and bottom depression pedons, respectively (Table 5). Since CEC depends on the nature and amount of soil colloids (Brady and Weil, 2008), the CEC of clay fraction can be used as a sign for the type of clay mineralogy (Buol et al., 2011). Thus, all soils are assumed to have smectite (60-100 cmolc kg^{-1}) clay group (Fekadu et al., 2018). Soils with high proportion of 2:1 expanding clay mineral, dominantly the montmorillonite (80-100 cmolc kg^{-1}), are also expected to reserve more Mg, K, and Fe nutrients (Landon, 2014). The percent base saturation (PBS) of the soils throughout the profiles ranged between 87.52 and 97.42 (Table 5). As per the rating of (Hazelton and Murphy, 2021), the PBS is under a very high (>80 %) category. The PBS values were higher in subsurface horizons than the surface, and the values in the surface horizons showed inconsistent decreasing and increasing trends along the toposequence. High values of PBS are in line with the high amount of Ca^{2+} occupying the exchange sites on the colloidal sites (Sekhar et al., 2014). The variation in PBS also indicates the degree of leaching which could be used as a diagnostic character for classifying soils (Meena et al., 2014).

The concentrations of DTPA extractable Fe, Mn, Zn, and Cu in the whole horizons varied from 0.1 to 5.36, 0.27 to 6.55, 0.01 to 0.95, and 0.05 to 0.25 mg kg^{-1} with inconsistent patter along the toposequence and with soil depth (Table 5). Generally, the highest concentrations of Fe, Mn, Zn, and Cu were recorded at the back-slope, bottom depression, foot-slope, and summit positions, respectively. Whereas, the lowest contents of the rest micro-nutrients existed at the summit position, except for Zn at the shoulder. Mn was followed by Fe, and both were the dominant cations in the surface soils of the profiles, except for the summit position (Table 5). As per the rating set by Wogi et al. (2021), the surface soils of the study area are under low to medium and medium to very high ranges in available Fe and Mn contents, respectively; but very low to low in available Zn and Cu contents.

The quantities of soil Fe, Mn, Zn, and Cu could be attributed to the vital factors like soil pH, OM content, clay amount and type, cation proportion, and drainage condition (Havlin et al., 2017). For instance, solubility and availability of Fe^{+3} in soil solution decreases a thousand-fold while that of Fe^{+2} and Mn^{+2} decreased by a hundred-fold for each unit increase in soil pH. Solution Fe and Mn ions are complexed by organic compounds in the soil solution which improves their availability through chelation reactions. Besides, soluble Fe and Mn concentrations could be increased under fine-textured and/or waterlogged soils that exhibit reduced O_2 and redox potential especially in lower pH condition. Havlin et al. (2017) also stated that Cu concentration is usually low at which most of the soluble Cu^{+2} in surface soils is organically complexed and strongly bound to OM than any other micronutrient. For soils with similar clay and OM contents, the role of OM to complexing of Cu is the highest with 1:1 versus 2:1 clays. The adsorption mechanism with oxides is unlike electrostatic attraction of Cu^{+2} on the CEC of clay particles, and involves in the formation of Cu-O-Fe/Al surface bonds (Havlin et al., 2017). A significant fraction of soil Cu is also occluded in various mineral structures, such as clay minerals and Fe, Al, and Mn oxides.

Table 5. Chemical properties of soils along the toposequence of Qenberenaweti sub-watershed

Profile	Horizon	Depth (cm)	pH (H_2O)	EC (ds/m)	OC	TN	Av. P	Ex. Ca	Ex. Mg	Ex. K	Ex. Na	CEC	CEC clay	BS	Av. Fe	Av. Mn	Av. Zn	Av. Cu
					%		Mgkg^{-1}	(cmol$_c$ kg^{-1})						(%)	(mg kg^{-1})			
Summit	A	0-25	5.59	0.155	1.83	0.17	18.82	29.38	6.14	0.91	0.16	41.20	72.72	90.27	2.17	1.63	0.41	0.08
	Bt1	25-70	6.23	0.358	0.43	0.07	22.74	23.08	11.92	0.84	0.21	40.76	54.55	90.28	1.45	1.36	0.19	0.11
	Bt2	70-105	7.17	0.293	0.51	0.08	15.32	23.14	11.76	0.81	0.25	40.80	52.74	90.29	0.18	0.57	0.33	0.08
	Btk1	105-135	7.18	0.391	0.38	0.04	4.24	28.40	13.02	0.78	0.32	48.59	70.05	89.90	0.10	0.36	0.45	0.05
	Btk2	135-165	6.97	0.452	0.76	0.04	10.39	32.26	7.50	0.73	0.36	46.84	71.29	89.97	0.17	0.37	0.01	0.13
	Btkm	165-200	7.65	0.280	0.29	0.03	6.33	18.46	21.30	0.86	0.37	47.03	64.96	89.99	0.17	0.27	0.23	0.05
Shoulder	A	0-30	6.23	0.087	1.67	0.16	15.69	22.72	11.08	0.66	0.15	39.45	73.26	89.05	3.22	5.95	0.12	0.17
	AB	30-65	6.52	0.096	1.04	0.12	20.62	19.78	11.12	0.92	0.17	36.55	63.42	89.25	3.82	2.00	0.36	0.12
	Bt1	65-100	6.06	0.287	0.78	0.09	13.25	18.63	12.67	0.91	0.20	37.15	52.23	89.21	1.28	1.56	0.30	0.09
	Bt2	100-120	6.38	0.395	0.27	0.03	4.92	22.15	12.26	0.81	0.24	40.82	55.42	89.00	0.37	1.03	0.18	0.07
	BC	120-135	6.77	0.145	0.31	0.02	3.35	23.55	7.62	0.54	0.28	36.99	69.10	89.24	0.48	1.01	0.16	0.08
Back slope	Ac1	0-20	5.97	0.259	1.69	0.14	22.89	14.37	23.14	0.41	0.19	40.77	83.16	95.14	4.50	5.92	0.22	0.16
	Ac2	20-40	5.95	0.198	1.52	0.13	24.27	13.01	24.46	0.37	0.17	40.59	80.30	95.15	3.99	1.55	0.03	0.14
	Bwv	40-60	5.31	0.409	0.22	0.02	12.28	11.35	20.81	0.52	0.20	35.19	74.83	95.51	4.53	2.16	0.40	0.12
	Bhsm	60-110	6.35	0.117	1.46	0.17	18.46	13.62	21.19	0.51	0.19	37.99	71.64	95.31	3.31	2.59	0.10	0.16
	Btx	110-125	5.93	0.346	0.86	0.08	10.08	19.24	21.57	0.60	0.19	44.56	67.07	94.93	1.84	1.81	0.27	0.12
	B/C	125-155	6.17	0.363	0.40	0.02	16.73	20.93	20.85	0.46	0.24	45.69	92.30	94.88	2.29	4.56	0.43	0.10
Foot slope	Ac1	0-35	5.63	0.143	1.80	0.18	11.49	19.78	18.58	0.42	0.16	42.44	86.30	93.07	2.89	4.32	0.18	0.18
	ABc2	35-70	6.41	0.187	1.71	0.17	13.57	20.94	19.36	0.41	0.18	43.71	99.47	95.08	5.09	3.86	0.64	0.15
	Btc3	70-95	5.94	0.165	1.56	0.15	11.61	19.64	18.12	0.54	0.21	42.17	65.72	93.10	4.27	3.30	0.95	0.14
	2Bti1	95-150	6.51	0.249	1.19	0.09	1.86	22.26	21.79	0.36	0.16	48.69	63.71	92.77	1.18	1.31	0.53	0.12
	2Bti2	150-200+	7.24	0.374	0.88	0.05	0.48	26.13	17.08	0.68	0.31	48.84	65.46	92.75	0.34	0.56	0.70	0.12
Toe slope	Ac1	0-20	6.32	0.143	2.03	0.18	23.96	20.96	8.04	0.72	0.18	31.45	58.24	97.14	3.37	5.82	0.21	0.15
	Ac2	20-45	5.61	0.091	1.53	0.13	16.38	28.01	2.86	0.45	0.16	33.07	63.17	97.01	3.42	5.51	0.75	0.11
	Ac3	45-70	5.87	0.243	1.69	0.17	19.20	10.80	16.20	0.58	0.16	29.07	52.80	97.42	5.36	4.58	0.01	0.25
	Bhc4	70-105	5.42	0.435	1.47	0.17	16.43	23.34	5.56	0.66	0.22	31.47	52.80	97.11	5.33	2.49	0.27	0.13
	B/C	105-165+	5.73	0.457	1.04	0.08	12.82	12.70	26.84	0.78	0.19	42.78	85.20	96.28	2.97	1.76	0.01	0.14
Bottom depression	Ag1	0-30	5.61	0.273	1.98	0.17	8.43	13.46	22.98	0.58	0.15	42.99	75.34	87.67	2.91	6.55	0.28	0.13
	Aqg2	30-65	6.69	0.119	1.43	0.16	8.53	21.78	17.44	0.72	0.14	46.38	82.93	87.52	2.24	4.94	0.38	0.15
	Bg3	65-110	6.16	0.058	0.84	0.14	15.64	26.12	5.86	0.49	0.18	37.86	64.73	88.01	3.82	2.71	0.21	0.11
	Bhg4	110-140	5.31	0.218	1.56	0.15	15.79	21.26	17.14	0.46	0.16	45.25	76.70	87.56	3.83	3.71	0.42	0.11
	BCg5	140-190	5.49	0.356	0.81	0.06	11.77	14.70	12.38	0.47	0.17	32.05	63.59	88.46	2.71	3.19	0.36	0.09

Similar to Cu^{+2}, soil solution Zn^{+2} is low as more than half of it creates stable complexes with high molecular weight organic compounds (lignin, humic acid and fulvic acid) that exist as soluble or insoluble forms. Typically, thirty-fold declines in solution Zn^{+2} due to complexation with organic matter have been observed for every unit pH increase between 5 and 7 (Havlin et al., 2017). Zn is also strongly adsorbed by magnesite, dolomite, and/or serpentine via getting into the crystal surface at sites normally occupied by Mg atoms (Havlin et al., 2017). Although the soils of the study area are not deficient in Fe and Mn, the low levels of available Zn and Cu indicate the potential deficiency of the elements. This finding is in line with Abayneh (2005) who reported Fe and Mn were at adequate levels across Ethiopian soils. Previous findings also indicated Zn and Cu deficiency in Ethiopian soils as a widespread problem (Ali et al., 2024; Karltun et al., 2013; Abayneh, 2005). All the micro-nutrients were positively correlated with OC content while they acquired negative correlations with soil pH. However, they were negatively related with clay particles and CEC except for the available Zn (Appendix Table 2).

Table 6. Values of selected soil chemical properties around excavated pedons

Pedons	Values	Properties								
		pH (H_2O)	OC (%)	TN (%)	Av.P (ppm)	Ex. K	Ex. Na	Ex. Ca	Ex. Mg	CEC
						($cmol_c\ kg^{-1}$)				
Summit	Mean	5.60	1.85	0.20	18.63	0.91	0.16	29.23	6.12	41.18
	SD	0.04	0.04	0.04	0.05	0.03	0.03	0.04	0.03	0.04
	CV (%)	0.71	2.16	20.00	0.27	3.30	18.75	0.14	0.49	0.10
Shoulder	Mean	6.22	1.67	0.14	15.82	0.68	0.14	22.67	11.13	39.46
	SD	0.05	0.06	0.05	0.13	0.07	0.03	0.10	0.12	0.11
	CV (%)	0.80	3.59	35.00	0.82	10.29	21.43	0.44	1.08	0.28
Back slope	Mean	5.94	1.71	0.13	22.79	0.44	0.18	14.35	23.18	40.91
	SD	0.06	0.08	0.04	0.15	0.03	0.04	0.10	0.12	0.12
	CV (%)	1.01	4.68	30.77	0.66	6.82	22.22	0.70	0.52	0.29
Foot slope	Mean	5.63	1.81	0.18	11.50	0.43	0.15	19.76	18.51	42.49
	SD	0.05	0.05	0.06	0.10	0.03	0.04	0.08	0.09	0.10
	CV (%)	0.89	2.76	33.33	0.87	6.98	26.67	0.40	0.49	0.24
Toe slope	Mean	6.20	2.01	0.16	23.98	0.75	0.19	20.97	8.04	31.41
	SD	0.04	0.04	0.03	0.04	0.03	0.03	0.02	0.03	0.03
	CV (%)	0.65	1.99	18.75	0.17	4.00	15.79	0.10	0.37	0.10
Depression	Mean	5.60	1.98	0.18	8.42	0.55	0.13	13.49	22.98	42.97
	SD	0.03	0.03	0.03	0.03	0.03	0.02	0.03	0.03	0.03
	CV (%)	0.54	1.52	16.67	0.36	5.45	15.39	0.22	0.13	0.07

Despite the higher SD value obtained at the back-slope position, there was low SD between the results in chemical properties of the surface soils of the horizons and their surrounding surface soils (Table 6). Apart from the intermediate variabilities (15 % < CV ≤ 35 %) in TN and exchangeable Na contents for surface horizons of the pedons and the corresponding surface soils around the pedons, the other chemical parameters showed similarities (CV < 15 %) among themselves at particular topographic positions (Wilding and Drees, 1978). Consequently, the soils of the surface horizons of the profile at a given topographic position represent the soils of their surrounding area.

Classification and Mapping of the Soils

Generally, the morphological and physicochemical properties of all the surface horizons were found within or very nearby the range of their concerned adjacent surface soil samples at a typical position of the toposequence. Similar to the pedons excavated and their surrounding surface soils, those SMUs having uniform/nearly closer results of common morphological (color, structure, consistence and texture-feel) and selected physicochemical properties (texture, pH, OC, basic cations and CEC) were considered and mapped as a similar soil group (Figure 4).

The soils of SMU 06 (the summit pedon), 09, 13, 18, and 29 were heavy textured blackish soils having a high proportion of alternatively shrink-swell clays which form wide deep cracks extending inward to ≥ 50 cm from the surface upon drying. The surface soils (≤ 30 cm) were evidenced by dusty appearance having a moist Munsell color value of ≤ 3 and chroma of ≤ 2. Besides, they had wedge-shaped aggregates with signs of frequent internal turnover (churning) of the soil materials below the upper 20 cm. Specifically, the summit pedon had thick (≥ 25 cm) subsurface horizons having more than 30 % clay and 80 % effective base saturation in 20-100 cm from the soil surface. About 80 % volume of the subsurface horizon between 25 and 70 cm depth was occupied by periodically broken wedge-shaped structural elements having an average horizontal length of < 10 cm. These properties qualify the soils for vertic diagnostic horizon. Moreover, there was a brownish subsurface horizon beyond the depth of 100 cm that has a clayey (≥ 30 %) texture with very firm and extremely hard consistencies when moist and dry, respectively, and produces effervescence when adding 1 M HCl due to its cementation by micro-crystalline forms of $CaCO_3$. Thus, such soils are classified as Pellic Bathypetroduric Vertisols (Hypereutric, Amphifractic) abbreviated as VR-pe-pdd-je-fcm.

Conversely, soils of SMU 02, 04, 05, 07, 08, 11, 12, 19, 26, and 28 exhibited wedge-shaped aggregates with a high proportion of alternatively shrink-swell clays that broke when dried, hence, qualified for vertic diagnostic horizons. However, these soils were at incipient stages of horizon differentiation which are evident from the changes in soil structure and color (mostly brownish discoloration) in their subsurface like that of the SMU 01, 03, 10, 14, 15, 16, 20, 21, 23, 24, 27, 30, 31, and 32. The soils were also characterized by slightly to moderately weathered medium and fine-textured materials, and the absence of considerable amounts of illuviated clay, organic matter, or Fe/Mn compounds within 100 cm from the soil surface. The shoulder pedon (SMU 05) was examined for the presence of ≥ 1 % soil organic carbon in the fine earth fraction of the upper two horizons to a weighted average depth of 65 cm with some noticeable soil structure and color changes from 30 to 65 cm because of a moderate pedogenetic alteration and wedge-shaped structural elements between a depth of 65 and 100 cm. Additionally, there were ≥ 30 % clay and 80 % effective base saturation throughout all horizons, hence, they are classified as Hypereutric Vertic Cambisols (Pantoclayic, Humic) abbreviated as CM-vr.je-cle-hu.

The soils of SMU 16 (the back-slope pedon), 01, 03, 10, 15, 20, 23, 24, and 27 were situated in human-made terraces, whereby ≥ 40 % of their soil surface was covered by fragments of ≥ 6 cm (stones and boulders) dimension. Also, their subsoils starting ≤ 100 cm from the soil surface had very to extremely hard and broken layer of indurated yellowish-brown materials which were cemented by Fe/Mn (hydr-) oxides with insignificant amount of organic matter. Particularly, the back-slope pedon was characterized by more than 40 % of interconnected yellowish-brown concretions and/or nodules of Fe/Mn (hydr-) oxides in reticulate patterns at which roots are only passing through vertical fractures of sheets having about 10 cm horizontal length at a depth of 40 to 60 cm. An illuvial accumulation of OM in the subsurface horizon was evident between the depths of 60 to 110 cm while having an iron-caused nearly continuous cementation. Besides, there was an illuvial accumulation of silicate clays with fragipan characteristics that developed a structure with a brittleness nature between 110 and 125 cm depth. All of the horizons throughout the pedon had clay content ≥ 30 %; with an effective base saturation (1 M

NH_4OAc, pH 7) of ≥ 80 %; soil organic carbon of ≥ 1 % in the fine earth fraction to a depth of 50 cm from the mineral soil surface; and an exchangeable Ca to Mg ratio of below 1 in the major part within 100 cm of the soil surface. Thus, all the diagnostic criteria qualified the soils for Hypereutric Akroskeletic Plinthofractic Cambisols (Pantoclayic, Escalic, Humic, Magnesic) abbreviated as CM-px.kk.je-cle.ec.hu.mg.

Although there was no evidence of advanced pedogenesis, appreciable signs of incipient weathering of primary minerals upon free internal and external drainages indicated the soils of SMU 32 (the toe-slope pedon), 14, 21, and 31 were at an early stage of soil formation. For instance, hydrolysis of iron-containing minerals (biotite, olivine, pyroxenes, and amphiboles) in a weakly acid environment produces ferrous iron that is oxidized to ferric oxides and hydroxides (goethite and haematite). This ‘free iron’ coated sand and silt particles and cemented clay, silt and sand into aggregates of yellowish-brown to reddish. There was some evidence of leaching of basic cations but no clear migration of Fe, organic matter, or clay was noted. The oxidative weathering process was not limited to the cambic horizon; rather, it also occurred in the surface A-horizon as the accumulated soil OM obscures its appearance. Explicitly, all horizons of the toe-slope pedon to a depth of 100 cm contained a pea-like yellowish, reddish, and/or blackish concretions or nodules of ≥ 2 mm diameter that were strongly cemented to indurated with Fe/Mn (hydr-) oxides in their ≥ 40 % volume. Moreover, all horizons throughout the pedon had clay contents higher than 30 % with an effective base saturation (1 M NH_4OAc, pH 7) of ≥ 80 % and soil organic carbon of ≥ 1.4 % in the fine earth fraction to a depth of 100 cm from the mineral soil surface. Consequently, the soils are grouped as Hypereutric Pisoplinthic Cambisols (Pantoclayic, Profundihumic) abbreviated as CM-px.je-cle.dh.

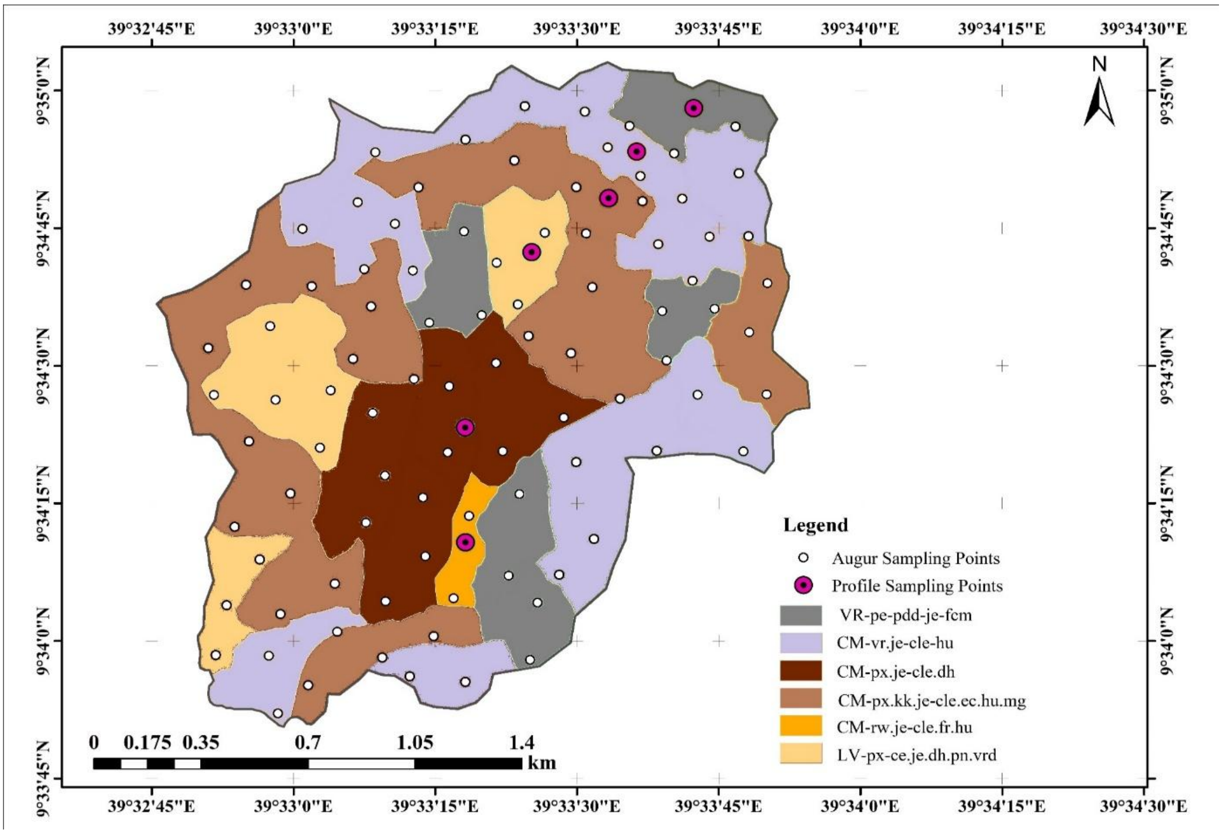

Figure 4. Soil map of the study area

The soils in the bottom depression pedon (SMU 30) had a layer ≥ 25 cm thick starting ≤ 75 cm from the mineral soil surface characterized by stagnic properties in which the area of reductimorphic colors plus the area of oximorphic colors are ≥ 25 % of the total layer area, and no reducing conditions. The segregation of ≥ 5 % reddish to blackish Fe and Mn oxides with a diameter of ≥ 2 mm in the subsurface horizon at a depth of 65 to 110 cm has taken place to such an extent that large mottles or discrete concretions or nodules were formed and the matrix between mottles, concretions or nodules were largely depleted of Fe and Mn. They did not have enhanced Fe and Mn contents, but Fe and Mn were concentrated in mottles or concretions, or nodules. Such segregation led to the poor aggregation of the soil particles in Fe- and Mn-depleted zones and compaction of the horizon. All horizons throughout the pedon had clay contents higher than 30 % with an effective base saturation (1 M NH_4OAc, pH 7) of ≥ 80 %; and soil organic carbon of ≥ 1 % in the fine earth fraction to a depth of 50 cm from the mineral soil surface. Hence, these soils are considered as Hypereutric Relictistagnic Cambisols (Pantoclayic, Ferric, Humic) abbreviated as CM-rw.je-cle.fr.hu.

The soils of SMU 17 (Foot-slope pedon), 22 and 25 had parent materials from colluvial deposition of different unconsolidated materials whereby higher clay content was noticed in the subsurface horizon that directly overlying coarser textured subsoil as a result of pedogenetic processes (especially clay migration) within the upper 100 cm. This condition made them satisfy the Argic principal qualifier listed under Luvisols. Principally, the foot-slope pedon was characterized by a pedogenetic clay differentiation with a lower clay content in the topsoil than in the subsoil without marked leaching of basic cations or advanced weathering of high-activity clays. The argic subsurface horizon existed directly below a coarser textured horizon, not separated by a lithic discontinuity between 70 and 95 cm deep at which its clay content did not decrease by ≥ 20 % (relative) from its maximum within 150 cm of the soil surface. The ratio of clay in the argic horizon to that of the coarser textured horizon was 1.47. In addition, more than 40 % of the subsurface soil volume was occupied by strongly cemented to indurated reddish and blackish pea-like concretions of Fe/Mn (hydr-) oxides with a diameter of ≥ 2 mm. The amount of OC in the fine earth fraction as a weighted average to a depth of 100 cm from the mineral soil surface was ≥ 1.4 % with an effective base saturation (1 M NH_4OAc, pH 7) of ≥ 80 % in layers between 20 and 100 cm from the mineral soil surface. The pedon had a texture class of clay, in a layer ≥ 30 cm thick within 100 cm of the mineral soil surface while the depth beyond a meter was attained by shiny-faced (slickensides) structures. Thus, these soils are grouped as Pisoplinthic Luvisols (Clayic, Hypereutric, Profundihumic, Profondic, Bathyvertic) abbreviated as LV-px-ce.je.dh.pn.vrd.

CONCLUSIONS

This study revealed that the nature and distribution of diversified soil types along the toposequence of the Qenberenaweti sub-watershed were influenced by the degree of variations in typical topographic positions and key slope features (steepness, aspect, and form). Because these pedogenesis factors directly affect the erosion-deposition and eluviation-illuviation of soil materials via controlling the action of water moving laterally across the surface and percolating vertically into the subsoils, respectively. Generally, the absence of inclusive evidence on the formation, development, and distribution of soils at a site-specific physiographic condition is often a constraint to the improvement of agriculture. Thus, the outputs of such detailed soil characterization, classification, and mapping work would give a vital clue for proper planning, management, and utilization of the soil resources at local topographic variability level. However, further research should be done to ensure sustainable agricultural production in the study area.

CONFLICTS OF INTEREST

Authors declare that they have no conflicts of interest.

ACKNOWLEDGEMENT

The authors would like to greatly acknowledge Hawassa University and Debre Berhan University for the overall assistance to conduct the study. Also, our sincere gratitude is extended to all individuals from various institutions who in one way or another contributed to the betterment of the study.

REFERENCES

Abate, N., & Kibret, K. 2016. Effects of land use, soil depth and topography on soil physicochemical properties along the toposequence at the Wadla Delanta Massif, Northcentral Highlands of Ethiopia. Environment and Pollution, 5(2): 57–71. [Scholar Google]

Abayneh, E. (2005). Characteristics, genesis and classification of reddish soils from Sidamo Region of Ethiopia. A PhD Dissertation, Putra Malaysia University.

Abdu, A., Laekemariam, F., Gidago, G., Kebede, A., & Getaneh, L. 2023. Variability analysis of soil properties, mapping, and crop test responses in Southern Ethiopia. Heliyon, 9(3). [Scholar Google]

Adhanom, D., & Toshome, T. 2016. Characterization and classification of soils of Aba-Midan sub watershed in Bambasi Wereda, West Ethiopia. International Journal of Scientific and Research Publications, 6(6): 390–399. [Scholar Google]

Adugna, G. 2016. A review on impact of compost on soil properties, water use and crop productivity. Academic Research Journal of Agricultural Science and Research, 4(3): 93–104. [Scholar Google]

Alemayehu, K., Sheleme, B., & Schoenau, J. 2016. Characterization of problem soils in and around the south central Ethiopian Rift Valley. Journal of Soil Science and Environmental Management, 7(11): 191–203. [Scholar Google]

Ali, A., Erkossa, T., Gudeta, K., Abera, W., Mesfin, E., Mekete, T., Haile, M., Haile, W., Abegaz, A., & Tafesse, D. 2024. Reference soil groups map of Ethiopia based on legacy data and machine learning-technique: EthioSoilGrids 1.0. Soil, 10(1): 189–209. [Scholar Google]

Ali, A., Esayas, A., & Beyene, S. 2010. Characterizing soils of Delbo Wegene watershed, Wolaita Zone, Southern Ethiopia for planning appropriate land management. Journal of Soil Science and Environmental Management, 1(8): 184–199. [Scholar Google]

Alves, G. B., Oliveira, F. S. de, Silva, A. H. N. da, & Souza, V. S. de. 2024. Toposequence: What are we talking about? Revista Brasileira de Ciência Do Solo, 48, e0230137. [Scholar Google]

Ande, O. T. 2010. Morphogenetic characterization of soils formed from basement complex rock in the humid tropical rainforest of Nigeria. Journal of Soil Science and Environmental Management, 1(6): 122–126. [Scholar Google]

ATDAO (Angolelana Tera district agricultural office). 2017. Community based watershed development planning. 29.

Ayalew, A., & Beyene, S. 2012. Characterization of soils at Angacha district in southern Ethiopia. Journal of Biology, Agriculture and Healthcare, 2(1): 2224–3208. [Scholar Google]

Ayalew, A., Beyene, S., & Walley, F. 2015. Characterization and classification of soils of selected areas in Southern Ethiopia. Journal of Environment and Earth Science, 5(11): 116–137. [Scholar Google]

Babalola, T. S., Fasina, A. S., & Tunku, P. 2007. Relationship between soil properties and slope position in a humid forest of South Western Nigeria. Medwell Online Agric. J, 2(3): 370–374. [Scholar Google]

Bedadi, B., Beyene, S., Erkossa, T., & Fekadu, E. 2023. Soil Management. In The Soils of Ethiopia (pp. 193–234). Springer. [Scholar Google]

Begna, M. 2020. Review on effect of toposequence on soil physicochemical properties. Ethiopian Journal of Environmental Studies & Management, 13(4). [Scholar Google]

Beyene, S. 2011. Characterization of Soils along a Toposequence in Gununo Area, Southern Ethiopia. Journal of Science and Development, 1(1): 31–41. [Scholar Google]

Bonfatti, B. R., Demattê, J. A. M., Marques, K. P. P., Poppiel, R. R., Rizzo, R., Mendes, W. de S., Silvero, N. E. Q., & Safanelli, J. L. 2020. Digital mapping of soil parent material in a heterogeneous tropical area. Geomorphology, 367, 107305. [Scholar Google]

Bouyoucos, G. J. 1951. A recalibration of the hydrometer method for making mechanical analysis of soils 1. Agronomy Journal, 43(9): 434–438. [Scholar Google]

Brady, N. C., & Weil, R. R. 2008. The Nature and Properties of Soils (14th ed.). Prentice Hall. https://books.google.com.et/books?id=73NFAAAAYAAJ. [Scholar Google]

Bremner, J. M., & Mulvany, C. S. 1982. Nitrogen total P. 595. 616. Methods of Soil Analysis".

Part2: Chemical and Microbiological Properties. Amer. Soc. of Agron., Inc., Madison, Wis., USA.

Brevik, E. C., Calzolari, C., Miller, B. A., Pereira, P., Kabala, C., Baumgarten, A., & Jordán, A. 2016. Soil mapping, classification, and pedologic modeling: History and future directions. Geoderma, 264: 256–274. [Scholar Google]

Buol, S. W., Southard, R. J., Graham, R. C., & McDaniel, P. A. 2011. Soil genesis and classification. John Wiley & Sons.

Chaplot, V. 2013. Impact of terrain attributes, parent material and soil types on gully erosion. Geomorphology, 186: 1–11. [Scholar Google]

Cherinet, A. 2017. Community perception on climate change, its impacts and adaptation strategies: the case of Ensaro woreda, North Shewa zone, amhara regional state, Ethiopia. In Thesis for in Partial Fulfilment of the Requirements for the Degree of Masters of Arts in Specialization of Climate Change and Adaptation Stream. Addis Ababa University Addis Ababa, Ethiopia.

Cools, N., & De Vos, B. 2010. Sampling and analysis of soil. Manual part X. Manual on Methods and Criteria for Harmonized Sampling, Assessment, Monitoring and Analysis of the Effects of Air Pollution on Forests. UNECE, ICP Forests, Hamburg, 208: 536–542.

Damene, S., Assen, M., & Esayas, A. 2007. Characteristics and classification of the soils of tenocha-wenchacher micro-catchment, South-west Shewa, Ethiopia. Ethiop J Nat Res. [Scholar Google]

Debele Bedane, M. 2018. Soil characterization, Classification, fertility mapping and physical land suitability evaluation for rain-fed production of major crops at muger sub-watershed, Northern Oromia, Ethiopia. Haramaya University. PhD Thesis.

Debele, M., Bedadi, B., Beyene, S., & Mohammed, M. 2018. Characterization and classification of soils of muger sub-watershed, northern oromia, Ethiopia. East African Journal of Sciences, 12(1): 11–28. [Scholar Google]

Deekor. T.N., A.I., I., F.O., O., S.O., A., & Ita. A.E. 2012). Changes in Soil Properties under Different Land Use Covers in Parts of Odukpani, Cross River State, Nigeria. Journal of Environment and Ecology, 3(1), 86–99. https://doi.org/10.5296/jee.v3i1.2265. [Scholar Google]

Dengiz, O. 2010. Morphology, physico-chemical properties and classification of soils on terraces of the Tigris River in the south-east Anatolia region of Turkey.

Dengiz, O., Saglam, M., Sarioglu, F. E., Saygin, F., & Atasoy, C. 2012. Morphological and physico-chemical characteristics and classification of vertisol developed on deltaic plain. Open Journal of Soil Science, 2(01): 20-27. [Scholar Google]

Deressa, A., Yli-Halla, M., Mohamed, M., & Wogi, L. 2018. Soil classification of humid Western Ethiopia: A transect study along a toposequence in Didessa watershed. Catena, 163: 184–195. [Scholar Google]

Dessalegn, D., Beyene, S., Ram, N., Walley, F., & Gala, T. S. 2014. Effects of topography and land use on soil characteristics along the toposequence of Ele watershed in southern Ethiopia. Catena, 115: 47–54. [Scholar Google]

Ditzler, C. A. 2017. Soil properties and classification (soil taxonomy). The Soils of the USA, 29–41.

Driessen, P., Deckers, J., Spaargaren, O., & Nachtergaele, F. 2000. Lecture notes on the major soils of the world. (Issue 94). Food and Agriculture Organization (FAO).

Driessen, P., Deckers, J., Spaargaren, O., & Nachtergaele, F. 2001. Lecture notes on the major soils of the world. Food and Agriculture Organization of the United Nations (FAO).

FAO. (2006). Guidelines For Field Soil Descriptions, Food and Agriculture Organization of the United Nations. (4th ed.).

Fekadu, E., Kibret, K., Bedadi, B., & Melese, A. 2018. Characterization and classification of soils of yikalo subwatershed in lay gayint district, northwestern highlands of Ethiopia. Eurasian Journal of Soil Science, 7(2): 151–166. [Scholar Google]

Gebrekidan, H., & Negassa, W. 2006. Impact of Land use and management practices on Chemical properties of some soils of Bako area, Western Ethiopia. Ethiopian Journal of Natural Resources. [Scholar Google]

Gérard, F. 2016. Clay minerals, iron/aluminum oxides, and their contribution to phosphate sorption in soils — A myth revisited. Geoderma, 262: 213–226. https://doi.org/https://doi.org/10.1016/j.geoderma.2015.08.036. [Scholar Google]

Gransee, A., & Führs, H. 2013. Magnesium mobility in soils as a challenge for soil and plant analysis, magnesium fertilization and root uptake under adverse growth conditions. Plant and Soil, 368: 5–21. [Scholar Google]

Gruber, F. E., Baruck, J., Mair, V., & Geitner, C. 2019. From geological to soil parent material maps-A random forest-supported analysis of geological map units and topography to support soil survey in South Tyrol. Geoderma, 354: 113884. [Scholar Google]

Hailu, A. H., Kibret, K., & Gebrekidan, H. 2015. Characterization and classification of soils of kabe subwatershed in south wollo zone, northeastern Ethiopia. African Journal of Soil Science, 3(7): 134–146. [Scholar Google]

Hartemink, A. E. 2015. The use of soil classification in journal papers between 1975 and 2014. Geoderma Regional, 5: 127–139. [Scholar Google]

Hartz, T. K. 2007. Soil testing for nutrient availability: procedures and interpretation for California vegetable crop production. Dept. of Plant Sciences: Davis, CA, USA.

Havlin, J. L., Tisdale, S. L., Nelson, W. L., & Beaton, J. D. 2017. Soil fertility and fertilizers. An Introduction to Nutrient Management. Pearson India Education Services Pvt. Ltd. Uttar Pradesh, India.

Hazelton, P., & Murphy, B. 2021. Understanding soils in urban environments. Csiro publishing.

IBM. 2020. SPSS survival manual: A step by step guide to data analysis using IBM SPSS. McGraw-hill education (UK).

IUSS. 2022. IUSS Working Group WRB.. World Reference Base for Soil Resources. International soil classification system for naming soils and creating legends for soil maps. 4 edition. International Union of Soil Sciences (IUSS), Vienna, Austria.

Jalali, M., & Arfania, H. 2010. Leaching of heavy metals and nutrients from calcareous sandy-loam soil receiving municipal solid sewage sludge. Journal of Plant Nutrition and Soil Science, 173(3): 407–416. https://doi.org/10.1002/jpln.200800225. [Scholar Google]

Jenny, H. 2012. The soil resource: origin and behavior (Vol. 37). Springer Science & Business Media.

Karltun, E., Mamo, T., Bekele, T., Gameda, S., & Kidanu, S. 2013. Towards improved fertilizer recommendations in Ethiopia—nutrient indices for categorization of fertilizer blends from EthioSISworeda soil inventory data. Addis Ababa, Ethiopia.

Khormali, F., Abtahi, A., Mahmoodi, S., & Stoops, G. 2003. Argillic horizon development in calcareous soils of arid and semiarid regions of southern Iran. Catena, 53(3): 273–301. [Scholar Google]

Kienast-Brown, S., Libohova, Z., & Boettinger, J. 2017. Digital soil mapping. Soil Survey Manual, 295–354.

Laekemariam, F., Kibret, K., Mamo, T., Karltun, E., & Gebrekidan, H. 2016. Physiographic characteristics of agricultural lands and farmers' soil fertility management practices in Wolaita zone, Southern Ethiopia. Environmental Systems Research, 5: 1–15. [Scholar Google]

Landon, J. R. 2014. Booker tropical soil manual: a handbook for soil survey and agricultural land evaluation in the tropics and subtropics. Routledge.

Lufega, S., & Msanya, B. 2017. Pedological characterization and soil classification of selected soil units of Morogoro District, Tanzania. International Journal of Plant & Soil Science, 16(1): 1–12. [Scholar Google]

Mathewos, M., & Mesfin, K. 2024. Characterization and classification of agricultural soils of Ajacho Lintala irrigation scheme, Soro district, Hadiya Zone, Southern Ethiopia. Sustainable Environment, 10(1): 2318054. [Scholar Google]

Meena, R. S., Natarajan, A., Thayalan, S., Hegde, R., Niranjana, K. V, Naidu, L. G. K., & Sarkar, D. 2014. Characterization and classification of lowland soils of Chikkarsinkere Hobli, Maddur taluk, Mandya district of Karnataka. Agropedology, 24(1): 95–101. [Scholar Google]

Megarsa, R. W. 2023. Characterization and classification of soils of hate leman micro-watershed in Dugda district, central Ethiopia. Haramaya University. MSc Thesis.

Mesfin, K., Tesfaye, S., Girma, K., Dejene, A., & Tsegaye, G. 2017. Description, characterization and classification of the major soils in Jinka Agricultural Research Center, South Western Ethiopia. Journal of Soil Science and Environmental Management, 8(3): 61–69. [Scholar Google]

Michael, A. M. 2009. Irrigation Theory And Practice - 2Nd Edn: Theory and Practice. Vikas Publishing House Pvt Limited. https://books.google.com.et/books?id=uDvuqawJDI4C

Minasny, B., & McBratney, A. B. 2016. Digital soil mapping: A brief history and some lessons. Geoderma, 264: 301–311. [Scholar Google]

MoARD (Ministry of Agriculture and Rural Development). 2005. Major agro-ecological zones of Ethiopia. In Forestry, Land Use and Soil Conservation Department. Addis Ababa.

Moradi, S. 2013. Impacts of organic carbon on consistency limits in different soil textures. International Journal of Agriculture and Crop Sciences, 5(12): 1381. [Scholar Google]

Mulugeta, D., & Sheleme, B. 2010. Characterization and classification of soils along the toposequence of Kindo Koye Watershed in Southern Ethiopia. East African Journal of Sciences, 4(2): 65–77. [Scholar Google]

Mulugeta, T., Melese, A., & Wondwosen, T. 2019. Effects of land use types on selected soil physical and chemical properties: The case of Kuyu District, Ethiopia. Eurasian Journal of Soil Science, 8(2) 94–109. [Scholar Google]

Mwendwa, S. 2021. Detailed Soil Survey and Spatial Variability of Selected Soil Properties in Upper Kabete Campus Field, University of Nairobi, Kenya. University of Nairobi. MSc Thesis.

Nahusenay, A., Kibebew, K., Heluf, G., & Abayneh, E. 2014. Characterization and classification of soils along the toposequence at the Wadla Delanta Massif, North Central Highlands of Ethiopia. Journal of Ecology and the Natural Environment, 6(9): 304–320. [Scholar Google]

Nega, E., & Heluf, G. 2009. Influence of land use changes and soil depth on cation exchange capacity and contents of exchangeable bases in the soils of Senbat Watershed, western Ethiopia. Ethiopian Journal of Natural Resources, 11(2): 195–206.

Newey, A. 2006. Litter carbon turnover with depth. Ph. D. Thesis, Australian National University, Canberra.

Nikiforova, A. A., Bastian, O., Fleis, M. E., Nyrtsov, M. V, & Khropov, A. G. 2019. Theoretical development of a natural soil-landscape classification system: An interdisciplinary approach. Catena, 177: 238–245. [Scholar Google]

Nyssen, J., Tielens, S., Gebreyohannes, T., Araya, T., Teka, K., Van de Wauw, J., Degeyndt, K., Descheemaeker, K., Amare, K., & Haile, M. 2019. Understanding spatial patterns of soils for sustainable agriculture in northern Ethiopia's tropical mountains. Plos One, 14(10): e0224041. [Scholar Google]

Ofori, E., Atakora, E. T., Kyei-Baffour, N., & Antwi, B. 2013. Relationship between landscape positions and selected soil properties at a Sawah site in Ghana. African Journal of Agricultural Research, 8(27): 3646–3652. [Scholar Google]

Ogban, P. I., Abang, P. O., Achi, E. A., & Nweke, C. 2019. Soil Management Systems Based on Soil Quality at Three Different Toposequences in Cross River State, South-Eastern Nigeria. Malaysian Journal of Soil Science, 23. [Scholar Google]

Omokaro, G. O. 2023. A Review on the Impacts of Toposequence on Soil Properties. American Journal of Environment and Climate, 2(3): 114–120. [Scholar Google]

Paltseva, A. 2024. What Are Soil Structure and Consistence? In The Urban Soil Guide: A Field and Lab Manual (pp. 31–34). Springer Nature.

Regassa, A., Assen, M., Ali, A., & Gessesse, B. 2023. Major soil types. In The Soils of Ethiopia (pp. 77–110). Cham: Springer International Publishing.

Richards, L. A., Allison, L., Bernstein, C. A., Bower, J. W., Brown, M., Fireman, J. T., Hatcher, H. ., Hayward, G. A., Pearson, R. C., Reeve, L. E., & Richards Wilcox, A. 1954. Diagnosis and Improvement of Saline and Alkali Soils (No. 60). US Government Printing Office.

Saha, A., Rattan, B., Sekharan, S., & Manna, U. 2020. Quantifying the interactive effect of water absorbing polymer (WAP)-soil texture on plant available water content and irrigation frequency. Geoderma, 368: 114310. [Scholar Google]

Schaetzl, R. J., & Thompson, M. L. 2015. Soils. Cambridge university press.

Seifu, W., & Elias, E. 2018. Soil quality attributes and their role in sustainable agriculture: a review. International Journal of Plant & Soil Science, 26(3): 1–26. [Scholar Google]

Seifu, W., Elias, E., Gebresamuel, G., Feyisa, G. L., & Tefera, W. 2023. Characterization and Mapping of Soil-Landscape for Site-Specific Soil Management in Ayiba Watershed, Northern Highlands of Ethiopia. Applied and Environmental Soil Science, 2023. [Scholar Google]

Sekhar, C. C., Balaguravaiah, D., & Naidu, M. V. S. 2014. Studies on genesis, characterization and classification of soils in central and Eastern parts of Prakasam district in Andhra Pradesh. Agropedology, 24(2): 125–137. [Scholar Google]

Senbayram, M., Gransee, A., Wahle, V., & Thiel, H. 2015. Role of magnesium fertilisers in agriculture: plant–soil continuum. Crop and Pasture Science, 66(12): 1219–1229. [Scholar Google]

Shahab, H., Emami, H., Haghnia, G. H., & Karimi, A. 2013. Pore size distribution as a soil physical quality index for agricultural and pasture soils in northeastern Iran. Pedosphere, 23(3): 312–320. [Scholar Google]

Shaw, R. J. 1999. Soil salinity—electrical conductivity and chloride. In 'Soil analysis—an interpretation manual'. (pp. 129–145). CSIRO Publishing: Melbourne.

Sheleme, B. 2017. Topographic positions and land use impacted soil properties along Humbo Larena-Ofa Sere toposequence, Southern Ethiopia. Journal of Soil Science and Environmental Management, 8(8): 135–147. [Scholar Google]

Sheleme, B. 2023. Introduction. The Soils of Ethiopia, 1–18.

Subhatu, A., Speranza, C. I., Zeleke, G., Roth, V., Lemann, T., Herweg, K., & Hurni, H. 2018. Interrelationships between terrace development, topography, soil erosion, and soil dislocation by tillage in Minchet Catchment, Ethiopian Highlands. Land Degradation & Development, 29(10): 3584–3594. [Scholar Google]

Taha, S. M., Mahmood, S. S., & Al Waeli, A. M. T. 2019. Preparation of mapping evaluation, extensional developmental agricultural chemical and fertility to soil using geographic information systems in Babylon governorate, Iraq. Plant Archives, 19(2): 3141-3150. [Scholar Google]

Tamene, L. D., Amede, T., Kihara, J. M., Tibebe, D., & Schulz, S. 2017. A review of soil fertility management and crop response to fertilizer application in Ethiopia: towards development of site-and context-specific fertilizer recommendation. CIAT Publication No. 443. International Center for Tropical Agriculture (CIAT), Addis Ababa, Ethiopia. 86p. Available at: http://hdl.handle.net/10568/82996.

Tan, K. H. 1995. Soil sampling, preparation, and analysis. CRC press.

Tardif, S., Cipullo, S., Sø, H. U., Wragg, J., Holm, P. E., Coulon, F., Brandt, K. K., & Cave, M. 2019. Factors governing the solid phase distribution of Cr, Cu and As in contaminated soil after 40 years of ageing. Science of the Total Environment, 652: 744–754. [Scholar Google]

Teshome, Y., Shelem, B., & Kibebew, K. 2016. Characterization and classification of soils of Abobo area, western Ethiopia. Applied and Environmental Soil Science, 2016. [Scholar Google]

Tufa, M., Fiseha, T., & Ahmed, S. 2021. Characterization and Classification of Soils of Askate Sub-watershed, South Wollo Zone, Northeastern Ethiopia. Journal of Biology, Agriculture and Healthcare, 11(3): 46-57. [Scholar Google]

Tunçay, T., & Dengiz, O. 2020. The roles of parent material and toposequence on geochemical characteristics and pedogenic iron oxides of soils. Indian Journal of Geo Marine Sciences, 49(4): 622-633. [Scholar Google]

Tursina, T. V. 2012. Approaches to the study of the lithological homogeneity of soil profiles and soil polygenesis. Eurasian Soil Science, 45: 472–487. [Scholar Google]

Van Ranst, E. 2006. Properties and management of soils in the tropics. Chapter, 2, 31–32.

Van Ranst, E., Verloo, M., Demeyer, A., & Pauwels, J. M. 1999. Manual for the soil chemistry and fertility laboratory: analytical methods for soils and plants equipment, and management of consumables.

Van Reeuwijk, L. P. 1995. Procedures for soil analysis. (No Title).

Wilding, L.P. and Drees , L.R. 1978 . " Spatial variability: A pedologist's viewpoint " . In Diversity of Soils in the Tropics , Edited by: Drosdoff , M. 1 – 12 . Madison , WI : American Society of Agronomy . ASA Special Publication Number 34. [Scholar Google]

Wimalasiri, E. M., Jahanshiri, E., Suhairi, T. A. S. T. M., Udayangani, H., Mapa, R. B., Karunaratne, A. S., Vidhanarachchi, L. P., & Azam-Ali, S. N. 2020. Basic soil data requirements for process-based crop models as a basis for crop diversification. Sustainability, 12(18): 7781. [Scholar Google]

Wogi, L., Dechassa, N., Haileselassie, B., Mekuria, F., Abebe, A., & Tamene, L. D. 2021. A guide to standardized methods of analysis for soil, water, plant, and fertilizer resources for data documentation and sharing in Ethiopia. CIAT Publication.

Yitbarek, T., Jembere, A., & Kerebeh, H. 2018. Characterization and classification of soils of Wolkite University research sites, Ethiopia. Eurasian Journal of Soil Science, 7(4): 292–299. [Scholar Google]

Zhu, J., Li, M., & Whelan, M. 2018. Phosphorus activators contribute to legacy phosphorus availability in agricultural soils: A review. Science of the Total Environment, 612: 522–537. https://doi.org/10.1016/j.scitotenv.2017.08.095. [Scholar Google]

APPENDIXES

Appendix Table 1. On-field topographic, physical and morphological properties of identified soil map units

SMU Id.	Slope (%)	Soil Depth (cm)	Soil Color (Munsell Code)		Surface Soil Texture (Feel)	Soil Consistency			
			Dry	Moist		Dry	Moist	Plasticity	Stickiness
SMU 01	15-30	50-100	Dark yellowish brown (10YR 3/6)	Very dark brown (7.5 YR 2.5/3)	Clay loam	SHA	VFR	SPL	SST
SMU 02	5-10	100-120	Very dark grayish brown (10YR 3/2)	Very dark gray (7.5 YR 3/1)	Clay	HA	FR	VPL	VST
SMU 03	15-30	50-100	Dark yellowish brown (10YR 3/4)	Very dark brown (7.5 YR 2.5/2)	Clay loam	SHA	VFR	PL	ST
SMU 04	5-10	>120	Dark brown (10YR 3/3)	Very dark brown (7.5 YR 2.5/2)	Clay loam	SHA	FR	PL	ST
SMU 05	10-15	100-120	Dark brown (10YR 3/3)	Very dark brown (7.5 YR 2.5/3)	Clay loam	SHA	VFR	VPL	ST
SMU 06	0-2	>120	Very dark grayish brown (10YR 3/2)	Very dark gray (7.5 YR 3/1)	Clay	VHA	VFR	PL	VST
SMU 07	2-5	>120	Dark yellowish brown (10YR 4/4)	Dark brown (7.5 YR 3/2)	Clay	SHA	VFR	PL	ST
SMU 08	10-15	100-120	Dark brown (10YR 3/3)	Very dark brown (7.5 YR 2.5/2)	Clay	SHA	FR	PL	ST
SMU 09	10-15	100-120	Dark yellowish brown (10YR 3/6)	Dark brown (7.5 YR 3/2)	Clay	HA	FR	VPL	VST
SMU 10	15-30	50-100	Dark yellowish brown (10YR 3/6)	Very dark brown (7.5 YR 2.5/2)	Clay loam	HA	FR	PL	ST
SMU 11	10-15	>120	Dark brown (10YR 3/3)	Very dark gray (7.5 YR 3/1)	Clay	VHA	FI	SPL	SST
SMU 12	15-30	100-120	Very dark grayish brown (10YR 3/2)	Very dark gray (7.5 YR 3/1)	Clay	VHA	FI	VPL	VST
SMU 13	15-30	100-120	Very dark brown (10YR 2/2)	Very dark brown (7.5 YR 2.5/2)	Clay	VHA	FR	VPL	VST
SMU 14	10-15	100-120	Dark yellowish brown (10YR 4/4)	Very dark brown (7.5 YR 2.5/2)	Clay loam	HA	FR	VPL	VST
SMU 15	15-30	50-100	Dark yellowish brown (10YR 3/4)	Very dark brown (7.5 YR 2.5/3)	Clay loam	HA	FR	PL	ST
SMU 16	15-30	100-120	Dark yellowish brown (10YR 3/4)	Very dark brown (7.5 YR 2.5/2)	Clay	SHA	VFR	PL	ST
SMU 17	10-15	100-120	Dark yellowish brown (10YR 4/4)	Dark brown (7.5 YR 3/3)	Clay loam	SHA	VFR	PL	ST
SMU 18	5-10	100-120	Dark yellowish brown (10YR 3/4)	Very dark brown (7.5 YR 2.5/3)	Clay	VHA	FI	VPL	VST
SMU 19	10-15	>120	Dark yellowish brown (10YR 3/4)	Dark brown (7.5 YR 3/2)	Clay	HA	FR	VPL	VST
SMU 20	15-30	50-100	Dark yellowish brown (10YR 3/6)	Very dark brown (7.5 YR 2.5/2)	Clay loam	SHA	VFR	SPL	SST
SMU 21	5-10	>120	Dark brown (10YR 3/3)	Dark brown (7.5 YR 3/2)	Clay loam	SHA	VFR	PL	ST
SMU 22	10-15	100-120	Dark brown (10YR 3/3)	Very dark brown (7.5 YR 2.5/2)	Clay loam	SHA	FR	PL	ST
SMU 23	15-30	50-100	Dark yellowish brown (10YR 4/4)	Dark brown (7.5 YR 3/2)	Clay loam	SHA	FR	PL	ST
SMU 24	15-30	50-100	Dark yellowish brown (10YR 4/4)	Dark brown (7.5 YR 3/2)	Clay loam	SHA	FR	PL	ST
SMU 25	10-15	100-120	Dark brown (10YR 3/3)	Dark brown (7.5 YR 3/3)	Clay loam	SHA	VFR	SPL	SST
SMU 26	5-10	100-120	Very dark grayish brown (10YR 3/2)	Very dark gray (7.5 YR 3/1)	Clay	HA	VFR	VPL	VST
SMU 27	15-30	50-100	Dark yellowish brown (10YR 3/4)	Dark brown (7.5 YR 3/2)	Clay loam	SHA	FR	PL	ST
SMU 28	5-10	>120	Dark yellowish brown (10YR 4/4)	Very dark brown (7.5 YR 2.5/2)	Clay loam	SHA	VFR	SPL	SST
SMU 29	5-10	100-120	Very dark grayish brown (10YR 3/2)	Very dark gray (7.5 YR 3/1)	Clay	VHA	FI	VPL	VST
SMU 30	2-5	>120	Dark yellowish brown (10YR 3/4)	Dark brown (7.5 YR 3/3)	Clay	HA	FR	VPL	ST
SMU 31	5-10	>120	Dark yellowish brown (10YR 4/4)	Very dark brown (7.5 YR 2.5/2)	Clay	SHA	VFR	PL	ST
SMU 32	5-10	>120	Dark yellowish brown (10YR 3/4)	Very dark brown (7.5 YR 2.5/3)	Clay	SHA	VFR	PL	ST

Appendix table 2. Correlation matrix for linear relationships between soil parameters

	Sand	Silt	Clay	pH	EC	OC	TN	Av.P	Ex. Na	Ex. K	Ex. Ca	Ex. Mg	CEC	Av. Fe	Av. Mn	Av. Cu	Av. Zn
Sand	1.00																
Silt	0.31	1.00															
Clay	-0.82***	-0.80***	1.00														
pH	-0.53**	-0.46**	0.61***	1.00													
EC	-0.18	-0.48**	0.40*	0.04	1.00												
OC	0.37*	0.69***	-0.65***	-0.45**	-0.52**	1.00											
TN	0.29	0.66***	-0.59***	-0.42*	-0.62***	0.93***	1.00										
Av.P	0.28	0.55**	-0.51**	-0.42*	-0.29	0.42*	0.50**	1.00									
Ex. Na	-0.55**	-0.42*	0.60***	0.71***	0.49**	-0.66***	-0.70***	-0.46**	1.00								
Ex. K	-0.40*	-0.42*	0.51**	0.39*	0.22	-0.32	-0.22	-0.04	0.34	1.00							
Ex. Ca	-0.48**	-0.15	0.39*	0.39*	-0.06	-0.16	-0.14	-0.25	0.40*	0.28	1.00						
Ex. Mg	0.22	-0.06	-0.10	-0.05	0.22	0.06	-0.05	-0.11	-0.11	-0.33	-0.70***	1.00					
CEC	-0.36*	-0.39*	0.46**	0.48**	0.21	-0.21	-0.30	-0.53**	0.39*	0.04	0.31	0.44*	1.00				
Av. Fe	0.61***	0.65***	-0.78***	-0.69***	-0.34	0.64***	0.67***	0.54**	-0.65***	-0.54**	-0.51**	0.16	-0.52**	1.00			
Av. Mn	0.61***	0.54**	-0.71***	-0.50**	-0.37*	0.65***	0.57***	0.44***	-0.60***	-0.57***	-0.44*	0.24	-0.30	0.70***	1.00		
Av. Cu	0.44*	0.52**	-0.59***	-0.34	-0.28	0.66***	0.64***	0.39	-0.53**	-0.38*	-0.42*	0.24	-0.31	0.71***	0.52**	1.00	
Av. Zn	-0.12	0.05	0.04	-0.08	-0.18	0.08	0.06	-0.20	-0.09	-0.19	0.26	-0.08	0.16	-0.01	0.11	-0.25	1.00

*** Very highly significant ($P \leq 0.001$), ** Highly significant ($P \leq 0.01$), * Significant ($P \leq 0.05$)

Note: The pair(s) of variables with positive correlation coefficients and P values below 0.05 tend to increase together. For the pairs with negative correlation coefficients and P values below 0.05, one variable tends to decrease while the other increases. For pairs with P values greater than 0.05, there is no significant relationship between the two variables.